6124 *Inorg. Chem.* **2010**, *49*, 6124–6138
DOI: 10.1021/ic1007395

Inorganic Chemistry
Article

Macrocyclic Gd^{3+} Chelates Attached to a Silsesquioxane Core as Potential Magnetic Resonance Imaging Contrast Agents: Synthesis, Physicochemical Characterization, and Stability Studies

Jörg Henig,[†] Éva Tóth,[‡] Jörn Engelmann,[§] Sven Gottschalk,[§] and Hermann A. Mayer*,[†]

[†]*Institut für Anorganische Chemie, Eberhard Karls Universität Tübingen, Auf der Morgenstelle 18, 72076 Tübingen, Germany,* [‡]*Le Centre de Biophysique Moléculaire, CNRS, Rue Charles Sadron, 45071 Orléans, France, and* [§]*Hochfeld-Magnetresonanz-Zentrum, Max-Planck-Institut für Biologische Kybernetik, Spemannstrasse 41, 72076 Tübingen, Germany*

Received April 16, 2010

Two macrocyclic ligands, 1,4,7,10-tetraazacyclododecane-1-glutaric-4,7,10-triacetic acid (H_5DOTAGA) and the novel 1,4,7,10-tetraazacyclododecane-1-(4-(carboxymethyl)benzoic)-4,7,10-triacetic acid (H_5DOTABA), were prepared and their lanthanide complexes (Ln = Gd^{3+}, Y^{3+}) attached to an amino-functionalized T_8-silsesquioxane. The novel compounds Gadoxane G (**GG**) and Gadoxane B (**GB**) possess eight monohydrated lanthanide complexes each, as evidenced by multinuclear (^{1}H, ^{13}C, ^{29}Si) NMR spectroscopy and high resolution mass spectrometry (HR-MS). Pulsed-field gradient spin echo (PGSE) diffusion ^{1}H NMR measurements revealed hydrodynamic radii of 1.44 nm and global rotational correlation times of about 3.35 ns for both compounds. With regard to potential MRI contrast agent applications, a variable-temperature ^{17}O NMR and ^{1}H nuclear magnetic relaxation dispersion (NMRD) study was carried out on aqueous solutions of the gadolinium(III) complexes of the Gadoxanes and the corresponding monomeric ligands to yield relevant physicochemical properties. The water exchange rates of the inner-sphere water molecules are all very similar (k_{ex}^{298} between $(5.3 \pm 0.5) \times 10^6$ s^{-1} and $(5.9 \pm 0.3) \times 10^6$ s^{-1}) and only slightly higher than that reported for the gadolinium(III) complex of 1,4,7,10-tetraazacyclododecane-1,4,7,10-tetraacetic acid (H_4DOTA) ($k_{ex}^{298} = 4.1 \times 10^6$ s^{-1}). Despite their almost identical size and their similar water exchange rates, **GB** shows a significantly higher longitudinal relaxivity than **GG** over nearly the whole range of magnetic fields (e.g., 17.1 mM^{-1} s^{-1} for **GB** and 12.1 mM^{-1} s^{-1} for **GG** at 20 MHz and 25 °C). This difference arises from their different local rotational correlation times ($\tau_{IR}^{298} = 240 \pm 10$ ps and 380 ± 20 ps, respectively), because of the higher rigidity of the phenyl ring of **GB** as compared to the ethylene spacer of **GG**. A crucial feature of these novel compounds is the lability of the silsesquioxane core in aqueous media. The hydrolysis of the Si−O−Si moieties was investigated by ^{29}Si NMR and PGSE diffusion ^{1}H NMR spectroscopy, electrospray ionization mass spectrometry (ESI-MS), as well as by relaxivity measurements. Although frozen aqueous solutions (pH 7.0) of **GG** and **GB** can be stored at −28 °C for at least 10 months without any decomposition, with increasing temperature and pH the hydrolysis of the silsesquioxane core was observed (e.g., $t_{1/2}$ = 15 h at pH 7.4 and 55 min at pH 8.1 for **GG** at 37 °C). No change in relaxivity was detected within the first 3 h, since the hydrolysis of the initial Si−O−Si moieties has no influence on the rotational correlation time. However, the further hydrolysis of the silsesquioxane core leads to smaller fragments and therefore to a decrease in relaxivity.

Introduction

The evolution of magnetic resonance imaging (MRI) to one of the most powerful tools in medical diagnosis is strongly related to the development of paramagnetic contrast agents (CAs). Most of the currently used CAs are stable chelates of trivalent gadolinium. Because of its seven unpaired electrons and slow electron spin relaxation, gadolinium(III) has a strong influence on the relaxation of surrounding water protons.[1−4] The CAs in clinical use today are mainly extracellular perfusion agents which distribute non-specifically throughout the plasma and the interstitial spaces. New CAs

*To whom correspondence should be addressed. E-mail: hermann.mayer@uni-tuebingen.de. Phone: +49 7071 29 76229. Fax: +49 7071 29 2436.

(1) *The Chemistry of Contrast Agents in Medical Magnetic Resonance Imaging*; É. Tóth, Merbach, A.E., Eds.; Wiley: Chichester, 2001.
(2) Aime, S.; Botta, M.; Fasano, M.; Terreno, E. *Chem. Soc. Rev.* **1998**, 19–29.
(3) Caravan, P.; Ellison, J. J.; McMurry, T. J.; Lauffer, R. B. *Chem. Rev.* **1999**, *99*, 2293–2352.
(4) Lauffer, R. B. *Chem. Rev.* **1987**, *87*, 901–927.

 Published on Web 06/08/2010

are continuously developed aiming at a more efficient and/or more specific imaging.[5] Relaxivity r_1, which measures the efficiency of a contrast agent, is defined as the paramagnetic longitudinal proton relaxation rate enhancement due to one millimolar concentration of the CA. The Solomon−Bloembergen−Morgan theory predicts that the relaxivity of a Gd^{3+}-based contrast agent can be improved with respect to that of current clinical agents by increasing the water exchange rate k_{ex} between the inner coordination sphere and the bulk water and by slowing down the rotational tumbling of the contrast agent.[3,6] A common way to obtain higher rotational correlation times, τ_R, is the attachment of low molecular weight Gd(III) chelates to macromolecules. Consequently, several approaches have been reported to optimize the rotational dynamics. These include covalent or noncovalent grafting of paramagnetic complexes to polymers,[7,8] dendrimers,[9,10] and biomolecules.[1,11,12] An alternative way to increase τ_R is through self-assembly of amphiphilic Gd(III) chelates to form micelles.[13,14] Given their higher relaxivity, significantly lower doses of the contrast agent could be used in MRI experiments. This aspect has become particularly important since the discovery of a correlation between nephrogenic systemic fibrosis (NSF) and some gadolinium based CAs.[15−17] High local gadolinium concentrations are also essential for the development of target specific CAs. Furthermore, their increased size prevents a leakage of the CAs into the interstitium and slows down the renal clearance from the body, thus allowing blood pool and tumor angiogenesis imaging.[18,19] Despite the advantages of macromolecular CAs, they have also a few drawbacks. Because of their slower excretion, the possibility to release toxic gadolinium(III) from the complexes, for example, by transmetalation, increases.[15,17,20,21] Moreover, macromolecular CAs, especially linear polymers, have usually poorly defined architectures, and their random morphology can lead to inconsistent and unpredictable pharmacokinetics. For micellar aggregates it is essential to maintain the monomer concentration in the body above the critical micelle concentration, which might prevent the application of lower concentrations of the CA in certain cases.[22] Dendrimeric macromolecules possess controllable molecular sizes and, at higher generations, a globular shape. However, even the large systems are often relatively flexible, and medium-sized dendrimeric contrast agents usually no longer have a well-defined three-dimensional structure.

Very recently, the first dendrimeric CAs having a symmetric T_8-silsesquioxane cube as the dendrimeric core have been reported.[23,24] Owing to its rigid three-dimensional structure the T_8-silsesquioxane core leads to compact globular CAs already at low generations. In the systems reported by Tanaka et al. the gadolinium(III) ions are directly coordinated via a carboxylic acid functionalized polyamidoamino (PAMAM) dendrimeric structure attached to each corner of the silsesquioxane. This leads to the complexation of two, four, and eight Gd^{3+} ions per molecule in the generations 1.5 to 3.5, respectively.[24] On the contrary, Kaneshiro et al. synthesized G1 to G3 poly-L-lysine dendrimers with an octa-(3-aminopropyl)silsesquioxane as the dendrimeric core and conjugated approximately 62−76% of the surface amine groups with Gd-DOTA-monoamide complexes.[23]

Today, high magnetic fields (above 3 T) are becoming more and more common not only in research but also in the clinics. The Solomon−Bloembergen−Morgan theory predicts that at such high magnetic fields, medium-sized CAs, like the metallostar compound of Livramento et al.,[25] are the most favored to achieve high relaxivities.

The aim of this work was therefore the development of small silsesquioxane-based CAs (Gadoxane G (**GG**) and Gadoxane B (**GB**), Figure 1), which still possess a large number of gadolinium(III) centers, embedded in well-defined macrocyclic ligand systems. Both Gadoxanes possess eight monohydrated lanthanide (Ln = Gd^{3+}, Y^{3+}) complexes, spherically arranged around the silsesquioxane core. Macrocyclic ligands were chosen, as their complexes show generally a much lower tendency to release gadolinium(III) via transmetalation than complexes of linear acyclic ligands.[20,21] The yttrium(III) analogues were synthesized to allow characterization of the compounds by means of NMR spectroscopy.

Pulsed-field gradient spin echo (PGSE) diffusion ^{1}H NMR spectroscopy was performed to obtain information about the molecular size of the Gadoxanes as well as of the monomeric complexes. Even though it is known that T_8-silsesquioxanes can undergo hydrolysis in aqueous media,[26] no investigations on the stability of the silsesquioxane core under physiological conditions have been reported for the previously mentioned silsesquioxane-based CAs.[23,24] This aspect, crucial for a potential silsesquioxane-based CA, was investigated in this study by NMR spectroscopy and mass spectrometry as well as by relaxivity measurements under physiological conditions. Furthermore, a variable-temperature ^{17}O NMR and ^{1}H nuclear magnetic relaxation dispersion (NMRD) study was carried out on the monomers and on the Gadoxanes,

(5) Lowe, M. P. *Aust. J. Chem.* **2002**, *55*, 551–556.
(6) Caravan, P. *Chem. Soc. Rev.* **2006**, *35*, 512–523.
(7) Dunand, F. A.; Tóth, É.; Hollister, R.; Merbach, A. *JBIC* **2001**, *6*, 247–255.
(8) Tóth, É.; Helm, L.; Kellar, K. E.; Merbach, A. *Chem.—Eur. J.* **1999**, *5*, 1202–1211.
(9) Nicolle, G. M.; Toth, E.; Schmitt-Willich, H.; Radüchel, B.; Merbach, A. E. *Chem.—Eur. J.* **2002**, *8*, 1040–1048.
(10) Tóth, É.; Pubanz, D.; Vauthey, S.; Helm, L.; Merbach, A. E. *Chem.—Eur. J.* **1996**, *2*, 1607–1615.
(11) Datta, A.; Hooker, J. M.; Botta, M.; Francis, M. B.; Aime, S.; Raymond, K. N. *J. Am. Chem. Soc.* **2008**, *130*, 2546–2552.
(12) Overoye-Chan, K.; Koerner, S.; Looby, R. J.; Kolodziej, A. F.; Zech, S. G.; Deng, Q.; Chasse, J. M.; McMurry, T. J.; Caravan, P. *J. Am. Chem. Soc.* **2008**, *130*, 6025–6039.
(13) André, J. P.; Tóth, É.; Fischer, H.; Seelig, A.; Mäcke, H. R.; Merbach, A. E. *Chem.—Eur. J.* **1999**, *5*, 2977–2983.
(14) Nicolle, G. M.; Tóth, É.; Eisenwiener, K.-P.; Mäcke, H. R.; Merbach, A. *JBIC* **2002**, *7*, 757–769.
(15) Aime, S.; Caravan, P. *J. Magn. Reson. Imaging* **2009**, *30*, 1259–1267.
(16) Grobner, T. *Nephrol., Dial., Transplant.* **2006**, *21*, 1104–1108.
(17) Sieber, M. A.; Pietsch, H.; Walter, J.; Haider, W.; Frenzel, T.; Weinmann, H.-J. *Invest. Radiol.* **2008**, *43*, 65–75.
(18) Lauffer, R. B.; Parmelee, D. J.; Dunham, S. U.; Ouellet, H. S.; Dolan, R. P.; Witte, S.; McMurry, T. J.; Walovitch, R. C. *Radiology* **1998**, *207*, 529–538.
(19) Lin, W.; Abendschein, D. R.; Celik, A.; Dolan, R. P.; Lauffer, R. B.; Walovitch, R. C.; Haacke, E. M. *J. Magn. Reson. Imaging* **1997**, *7*, 963–971.
(20) Idée, J.-M.; Port, M.; Raynal, I.; Schaefer, M.; Le Greneur, S.; Corot, C. *Fundam. Clin. Pharmacol.* **2006**, *20*, 563–576.
(21) Idée, J.-M.; Port, M.; Robic, C.; Medina, C.; Sabatou, M.; Corot, C. *J. Magn. Reson. Imaging* **2009**, *30*, 1249–1258.
(22) Torres, S.; Martins, J. A.; André, J. P.; Geraldes, C. F. G. C.; Merbach, A. E.; Tóth, É. *Chem.—Eur. J.* **2006**, *12*, 940–948.
(23) Kaneshiro, T. L.; Jeong, E.-K.; Morrell, G.; Parker, D. L.; Lu, Z.-R. *Biomacromolecules* **2008**, *9*, 2742–2748.
(24) Tanaka, K.; Kitamura, N.; Naka, K.; Morita, M.; Inubushi, T.; Chujo, M.; Nagao, M.; Chujo, Y. *Polym. J.* **2009**, *41*, 287–293.
(25) Livramento, J. B.; Sour, A.; Borel, A.; Merbach, A. E.; Tóth, É. *Chem.—Eur. J.* **2006**, *12*, 989–1003.
(26) Feher, F. J.; Wyndham, K. D. *Chem. Commun.* **1998**, 323–324.

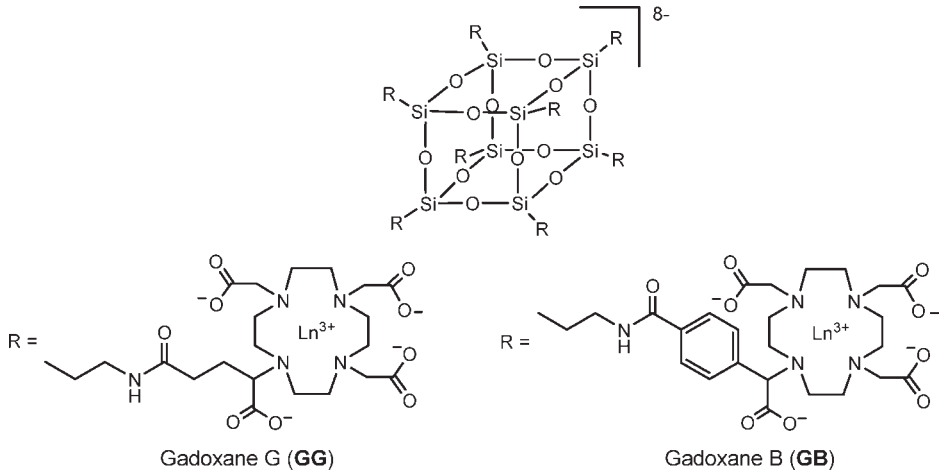

Figure 1. Gadoxane G (**GG**) and Gadoxane B (**GB**).

which is the first physicochemical characterization of silsesquioxane-based gadolinium compounds for potential application as an MRI CA.

Experimental Section

Materials and Methods. Column chromatography was performed using silicagel 60. All chemicals were used as purchased. Diafiltration was carried out on a Pall Minimate Tangential Flow Filtration System using a Pall Minimate TFF Capsule with an Omega 3K PES ultrafiltration membrane. ^{1}H, ^{13}C{^{1}H}, and ^{29}Si{^{1}H} NMR spectra were recorded on a Bruker Avance II 400 MHz or a Bruker Avance II^{+} 500 MHz spectrometer at room temperature, unless otherwise specified. ^{1}H and ^{13}C NMR resonances were assigned using standard 2D techniques (^{1}H−^{1}H COSY, ^{1}H−^{13}C HSQC, ^{1}H−^{13}C HMBC). Except for ^{1}H NMR spectra measured in D_2O, which were referenced to the residual HDO peak (δ = 4.79), all ^{1}H, ^{13}C{^{1}H}, and ^{29}Si{^{1}H} NMR spectra were externally referenced to 1% TMS in $CDCl_3$ via deuterium lock.[27] Elemental analysis was performed on an Elementar vario MICRO cube elemental analyzer. HR mass spectra were recorded on a Bruker Daltonics 4.7 T APEX II FT-ICR instrument equipped with an electrospray ionization (ESI) source. In the positive mode appropriate polyethylene glycol molecules were used for internal calibration and perfluoroheptanoic acid, perfluorooctanoic acid, perfluorodecanoic acid, and perfluorododecanoic acid were used in the negative mode. pH and pD[28] values of aqueous solutions were measured using a Schott handylab pH12 pH-meter equipped with a Mettler−Toledo Inlab Micro glass electrode.

Ligand Synthesis. 2-Bromoglutaric Acid. To a stirred solution of L-glutamic acid (**4**) (16.50 g, 112 mmol) and sodium bromide (40.00 g, 389 mM) in aqueous 2 N hydrobromic acid (100 mL) cooled to 0 °C sodium nitrite (14.00 g, 203 mM) was added gradually over a period of 2 h. About 10 min after the last addition conc. sulfuric acid (6 mL) was added. The mixture was extracted three times with diethyl ether. The combined organic phases were washed with brine and dried over magnesium sulfate. Removal of the solvent under reduced pressure resulted in a yellow oil (11.13 g, 47%, about 85% pure). ^{1}H NMR (400.13 MHz, $CDCl_3$): δ = 9.99 (br s, 2H, COO*H*), 4.42 (dd, $^{3}J_{HH}$ = 7.3 Hz, $^{3}J_{HH}$ = 6.2 Hz, 1H, C*H*Br), 2.73−2.60 (m, 2H, CH_2COOH), 2.49−2.27 (m, 2H, CHBrCH_2). ^{13}C{^{1}H} NMR (100.61 MHz, $CDCl_3$): δ = 178.8 (CH_2*C*OOH), 175.0 (CHBr*C*OOH), 44.1 (*C*HBr), 31.3 (*C*H_2COOH), 29.3 (CHBr*C*H_2).

Dimethyl 2-Bromoglutarate (5). The crude 2-bromoglutaric acid (5.00 g, ∼20 mmol) was dissolved in a solution of conc. sulfuric acid (700 μL) in methanol (50 mL), and the mixture was heated to reflux for 1 h. The solution was allowed to reach room temperature and concentrated under reduced pressure. Diethyl ether was added, and the organic phase was washed with aqueous $NaHCO_3$ (5%) followed by brine and dried over magnesium sulfate. After removal of the solvent under reduced pressure, the crude product was purified on a short silica gel column (*n*-hexane/ethyl acetate 9:1) resulting in a colorless oil (3.60 g, 75%). ^{1}H NMR (400.13 MHz, $CDCl_3$): δ = 4.32 (dd, $^{3}J_{HH}$ = 8.4 Hz, $^{3}J_{HH}$ = 5.8 Hz, 1H, C*H*Br), 3.72 (s, 3H, CH_2COOCH_3), 3.63 (s, 3H, CHBrCOOCH_3), 2.54−2.40 (m, 2H, CH_2COOCH_3), 2.38−2.16 (m, 2H, CHBrCH_2). ^{13}C{^{1}H} NMR (100.61 MHz, $CDCl_3$): δ = 172.4 (CH_2*C*OOCH$_3$), 169.8 (CHBr*C*OOCH$_3$), 53.0 (CH_2COO*C*H$_3$), 51.8 CHBrCOO*C*H$_3$), 44.6 (*C*HBr), 31.2 (*C*H_2COOCH$_3$), 29.7 (CHBr*C*H_2). Anal. Calcd for $C_7H_{11}BrO_4$: C, 35.17, H, 4.64, found: C, 35.13, H, 4.38.

4-(Carboxymethyl)benzoic Acid (7). The title compound was prepared from methyl 4-(cyanomethyl)-benzoate (**6**) according to the literature[29] in 84% yield.

Methyl 4-((methoxycarbonyl)methyl)benzoate (8). Under argon atmosphere **7** (1.00 g, 5.55 mmol) was dissolved in dry methanol (20 mL) and cooled to 0 °C. A solution of thionyl chloride (1 mL, 13.78 mmol) in dry methanol (20 mL) was added dropwise over 15 min. The solution was allowed to reach room temperature and stirred for 22 h. Removal of the volatile matter under reduced pressure resulted in a yellow oil (1.10 g, 95%). ^{1}H NMR (400.13 MHz, $CDCl_3$): δ = 8.00 (m, A-portion of an $[AB]_2$-system, 2H, Ar-2-H, Ar-6-H), 7.37 (m, B-portion of an $[AB]_2$-system, 2H, Ar-3-H, Ar-5-H), 3.67 (s, 2H, CH_2), 3.90 (s, 3H, ArCOOCH_3), 3.69 (s, 3H, CH_2COOCH_3). ^{13}C{^{1}H} NMR (100.61 MHz, $CDCl_3$): δ = 171.1 (CH_2*C*OOCH$_3$), 166.7 (Ar*C*OOCH$_3$), 138.8 (Ar-4-C), 129.8 (Ar-2-C, Ar-6-C), 129.3 (Ar-3-C, Ar-5-C), 128.9 (Ar-1-C), 52.5 (CH_2COO*C*H$_3$), 52.4 ArCOO*C*H$_3$), 41.2 (*C*H_2).

Methyl 4-((methoxycarbonyl)bromomethyl)benzoate (9). Under argon atmosphere *N*-bromosuccinimide (NBS) (0.970 g, 5.450 mmol) and azobisisobutyronitrile (AIBN) (50 mg, 0.304 mmol) were added to a solution of **8** (1.075 g, 5.163 mmol) in freshly distilled carbon tetrachloride (20 mL). The mixture was heated to reflux for 5 h, after which the ^{1}H NMR spectrum indicated only 49% conversion. Therefore, new AIBN (50 mg, 0.304 mmol) was added, and the mixture was refluxed for additional 17 h. The white solid was filtered off, and the solvent

(27) Gottlieb, H. E.; Kotlyar, V.; Nudelman, A. *J. Org. Chem.* **1997**, *62*, 7512–7515.
(28) Glasoe, P. K.; Long, F. A. *J. Phys. Chem.* **1960**, *64*, 188–190.
(29) Schaper, K.; Mobarekeh, S. A. M.; Grewer, C. *Eur. J. Org. Chem.* **2002**, *2002*, 1037–1046.

removed under reduced pressure. The crude product (73% due to ^{1}H NMR) was purified on a silica gel column (*n*-hexane/ethyl acetate 3:1) resulting in a colorless oil (711 mg, 48%). ^{1}H NMR (250.13 MHz, $CDCl_3$): δ = 8.04 (m, A-portion of an $[AB]_2$-system, 2H, Ar-2-H, Ar-6-H), 7.63 (m, B-portion of an $[AB]_2$-system, 2H, Ar-3-H, Ar-5-H), 5.39 (s, 1H, C*H*Br), 3.93 (s, 3H, ArCOOCH_3), 3.81 (s, 3H, CHBrCOOCH_3). ^{13}C{^{1}H} NMR (62.90 MHz, $CDCl_3$): δ = 168.4 (CHBr*C*OOCH$_3$), 166.3 (Ar*C*OOCH$_3$), 140.5 (Ar-4-C), 130.9 (Ar-1-C), 130.0 (Ar-2-C, Ar-6-C), 128.7 (Ar-3-C, Ar-5-C), 53.6 (CHBrCOO*C*H$_3$), 52.3 ArCOO*C*H$_3$), 45.4 (*C*HBr). Anal. Calcd for $C_{11}H_{11}BrO_4$: C, 46.02, H, 3.84, found: C, 46.22, H, 3.54.

General Procedure for the Synthesis of 11 and 12. Under argon atmosphere tri-*tert*-butyl 1,4,7,10-tetraazacyclododecane-1,4,7-triacetate (**10**) (1 equiv) was dissolved in dry acetonitrile (25 mL) and **5** or **9** (1.1 equiv) was added, followed by K_2CO_3 (1.5 equiv). The mixture was stirred for 17 h at 70 °C. After cooling to room temperature, the solid was filtered off, and the solvent removed under reduced pressure. The crude product was purified on a silica gel column (pure $CHCl_3$, gradually increasing the ratio of MeOH to 15% for **11** and 10% for **12**).

1,4,7,10-Tetraazacyclododecane-1-glutaric Acid Methyl Diester-4,7,10-triacetic Acid *tert*-Butyl Ester (11). Yellow solid, 71% yield. ^{1}H NMR (500.13 MHz, $CDCl_3$): δ = 3.59 (s, 3H, NCHCOOCH_3), 3.53 (s, 3H, $CH_2CH_2COOCH_3$), 3.48 (dd, $^3J_{HH}$ = 10.3 Hz, $^3J_{HH}$ = 2.4 Hz, 1H, NC*H*COOCH$_3$), 3.32 (d, $^2J_{HH}$ = 17.3 Hz, 1H, NC*H*HCOO^{t}Bu), 2.73 (d, $^2J_{HH}$ = 17.3 Hz, 1H, NCH*H*COO^{t}Bu), 3.27 (d, $^2J_{HH}$ = 17.6 Hz, 1H, NC*H*-HCOO^{t}Bu), 2.74 (d, $^2J_{HH}$ = 17.6 Hz, 1H, NCH*H*COO^{t}Bu), 3.27 (d, $^2J_{HH}$ = 17.0 Hz, 1H, NC*H*HCOO^{t}Bu), 2.72 (d, $^2J_{HH}$ = 17.0 Hz, 1H, NCH*H*COO^{t}Bu), 3.08, 2.05 (br m, 6H, Cyclen CH_2), 2.96, 2.37 (br m, 2H, Cyclen CH_2), 2.49 (m, 2H, CH_2CH_2COOCH$_3$), 2.43, 2.25 (br m, 4H, Cyclen CH_2), 2.41, 2.25 (br m, 2H, Cyclen CH_2), 1.92, 1.68 (m, 2H, CH_2-CH_2COOCH$_3$), 1.34 (s, 9H, C(CH_3)$_3$), 1.33 (s, 9H, C(CH_3)$_3$), 1.31 (s, 9H, C(CH_3)$_3$). ^{13}C{^{1}H} NMR (125.76 MHz, $CDCl_3$): δ = 175.9 (NCH*C*OOCH$_3$), 173.2 (CH_2CH_2*C*OOCH$_3$), 173.0, 172.9, 172.7 (NCH$_2$*C*OO^{t}Bu), 82.0, 81.90, 81.86 (*C*(CH$_3$)$_3$), 59.2 (*C*HCOOCH$_3$), 55.7, 55.6, 55.4 (N*C*H$_2$COO^{t}Bu), 52.6, 52.5, 52.3, 48.5, 48.4, 48.0, 47.0, 44.6 (Cyclen *C*H$_2$), 52.1 (NCH-COO*C*H$_3$), 51.5 (CH_2CH_2COO*C*H$_3$), 31.6 (CH_2*C*H$_2$COOCH$_3$), 27.73, 27.72, 27.68, (C(*C*H$_3$)$_3$), 19.0 (*C*H$_2$CH$_2$COOCH$_3$). HRMS (FTICR): $[M+Na]^+$ calcd: 695.42017, found: 695.42074.

1,4,7,10-Tetraazacyclododecane-1-(4-(carboxymethyl)benzoic) Acid Methyl Diester-4,7,10-triacetic Acid *tert*-Butyl Ester (12). Off-white powder, 86% yield. ^{1}H NMR (500.13 MHz, $CDCl_3$): δ = 8.00 (m, A-portion of an $[AB]_2$-system, 2H, Ar-2-H, Ar-6-H), 7.11 (m, B-portion of an $[AB]_2$-system, 2H, Ar-3-H, Ar-5-H), 4.72 (s, 1H, C*H*COOCH$_3$), 3.89 (s, 3H, ArCOOCH_3), 3.67 (s, 3H, CHCOOCH_3), 3.56 (d, $^2J_{HH}$ = 17.4 Hz, 1H, NC*H*HCOO^{t}Bu), 2.87 (d, $^2J_{HH}$ = 17.4 Hz, 1H, NCH*H*COO^{t}Bu), 3.41 (d, $^2J_{HH}$ = 17.5 Hz, 1H, NC*H*HCOO^{t}Bu), 2.94 (d, $^2J_{HH}$ = 17.5 Hz, 1H, NCH*H*COO^{t}Bu), 3.37 (d, $^2J_{HH}$ = 17.3 Hz, 1H, NC*H*HCOO-^{t}Bu), 2.83 (d, $^2J_{HH}$ = 17.3 Hz, 1H, NCH*H*COO^{t}Bu), 3.34, 2.22 (m, 2H, Cyclen CH_2), 3.27, 2.12 (m, 2H, Cyclen CH_2), 3.24, 2.09 (m, 2H, Cyclen CH_2), 3.17, 2.25 (m, 2H, Cyclen CH_2), 2.86, 1.71 (m, 2H, Cyclen CH_2), 2.71, 2.52 (m, 2H, Cyclen CH_2), 2.51, 2.35 (m, 2H, Cyclen CH_2), 2.50, 2.36 (m, 2H, Cyclen CH_2), 1.46, 1.43 (overl. s, 27H, C(CH_3)$_3$). ^{13}C{^{1}H} NMR (125.76 MHz, $CDCl_3$): δ = 174.7 (CH*C*OOCH$_3$), 173.9, 173.3, 173.1 (*C*OO^{t}Bu), 166.5 (Ar*C*OOCH$_3$), 136.9 (Ar-4-C), 130.3 (Ar-1-C), 130.1 (Ar-3-C, Ar-5-C), 129.7 (Ar-2-C, Ar-6-C), 82.5, 82.2, 82.1 (*C*(CH$_3$)$_3$), 65.0 (*C*HCOOCH$_3$), 56.1, 55.9, 55.6 (*C*H$_2$COO^{t}Bu) 52.9, 52.6, 52.5, 49.0, 48.5, 48.3, 48.1, 45.1 (Cyclen *C*H$_2$), 52.6 (CHCOO*C*H$_3$), 52.3 (ArCOO*C*H$_3$), 28.1, 28.0, 27.9 (C(*C*H$_3$)$_3$). HRMS (FTICR): $[M+Na]^+$ calcd: 743.42017, found: 743.42024.

General Procedure for the Synthesis of 2 and 3. **11** or **12** was dissolved in aqueous 6 N hydrochloric acid (30 mL) and refluxed for 17 h. The solution was allowed to reach room temperature, washed with diethyl ether, and the solvent removed under reduced pressure to yield the ammonium chloride salt of **2** or **3** (containing about 85% pure ligand).

1,4,7,10-Tetraazacyclododecane-1-glutaric-4,7,10-triacetic Acid (2). Off-white powder, 92% yield. ^{1}H NMR (400.13 MHz, D_2O): δ = 3.99 (dd, $^3J_{HH}$ = 9.0 Hz, $^3J_{HH}$ = 3.8 Hz, 1H, NC*H*COOH), 3.95−2.90 (br, 22H, NCH_2), 2.68 (m, 2H, CH_2CH_2COOH), 2.01 (m, 2H, CH_2CH_2COOH). ^{13}C{^{1}H} NMR (100.61 MHz, D_2O): δ = 177.4 (CH_2CH_2*C*OOH), 175.2, 174.0, 170.4 (br, NCH$_2$-*C*OOH), 59.6 (br, *C*HCOOH), 55.9, 53.8, 51.0, 48.5, 45.6, 44.3 (br, N*C*H$_2$), 31.4 (CH_2*C*H$_2$COOH), 21.7 (*C*H$_2CH_2$COOH). HRMS (FTICR): $[M+H]^+$ calcd: 477.21912, found: 477.21900.

1,4,7,10-Tetraazacyclododecane-1-(4-(carboxymethyl)benzoic)-4,7,10-triacetic Acid (3). Off-white powder, 90% yield. ^{1}H NMR (500.13 MHz, D_2O): δ = 8.01(m, A-portion of an $[AB]_2$-system, 2H, Ar-2-H, Ar-6-H), 7.55 (br m, B-portion of an $[AB]_2$-system, 2H, Ar-3-H, Ar-5-H), 5.45 (br s, 1H, C*H*COOH), 4.63−2.38 (br, 22H, CH_2). ^{13}C{^{1}H} NMR (125.76 MHz, D_2O): δ = 174.9, 173.5, 168.9, 167.8 (extr. br) (*C*OOH), 169.6 (Ar*C*OOH), 138.4 (Ar-4-C), not observed (Ar-1-C), 130.5 (Ar-2-C, Ar-6-C), 130.4 (Ar-3-C, Ar-5-C), 63.3 (*C*HCOOH), 54.9, 53.2, 52.0(br), 51.2-(br), 50.0−46.1(extr. br), 45.6, 43.3 (*C*H$_2$). HRMS (FTICR): $[M+H]^+$ calcd: 525.21912, found: 525.21938.

Octa(3-chloroammoniumpropyl)silsesquioxane (15). 15 was synthesized according to the literature[26] procedure in 39% yield.

Synthesis of the Gadoxanes. Ligand **2** (49 mg, 8.74×10^{-5} mol, for **GG**) or ligand **3** (65 mg, 1.02×10^{-4} mol, for **GB**) was dissolved in an aqueous solution of *n*-Bu$_4$NOH (20%, 548 μL, 4.18×10^{-4} mol for **GG**; 20%, 802 μL, 6.12×10^{-4} mol, for **GB**) followed by the addition of 1.1 equiv of a stock solution of $LnCl_3$. The pH was verified to be between 6 and 7. The solution/suspension was heated to 70 °C for about 3 h. The solvent was removed under reduced pressure, and the remaining solid residue was dried for 4 to 6 days in vacuo. Under argon atmosphere the residue was taken up in dry DMSO (1 mL for **GG** and 5 mL for **GB**) and stirred for 1 day. To the resulting solution octa(3-chloroammoniumpropyl)silsesquioxane (**15**), dissolved in dry DMSO (10 mg, 8.51×10^{-6} mol in 0.5 mL dry DMSO), was added, followed by DIPEA (0.1 mL, 5.84×10^{-4} mol) and TBTU (33 mg, 1.02×10^{-4} mol). After 30 min/3 h (**GG**/**GB**) of stirring at room temperature the reaction mixture was added dropwise to an acetic acid/sodium acetate buffer (buffer capacity of 12 mmol/L, pH 5.5, 50 mL). This solution was poured into 50 mL of distilled water in the reservoir of a Pall Minimate Tangential Flow Filtration System. Diafiltration was carried out using a membrane with a molecular weight cutoff of 3K. The permeated volume was continuously replaced by an aqueous solution of NaCl (1%, 400 mL), followed by pure water (400 mL). After the volume replacement was stopped, the diafiltration was continued until the volume had reduced to about 10 mL. The remaining solution was collected in a Schlenk flask (rinsed with 10 mL H_2O). The solvent was removed in vacuo at 25 °C to afford **GG** or **GB** as a colorless solid. The yield calculated from the gadolinium(III) concentration obtained by the BMS method[30] was about 37% for **GG** and 30% for **GB**. The absence of non-coordinated lanthanide ions was confirmed by the xylenol test.[31]

Characterization data of the yttrium complex of **GG**: ^{1}H NMR (500.13 MHz, D_2O,): δ = 3.63 (br d, 16H, C*H*HCOO$^-$), 3.25 (br d, 16H, CH*H*COO$^-$), 3.63 (br d, 8H, C*H*HCOO$^-$), 3.22 (br d, 8H, CH*H*COO$^-$), 3.48, 2.47 (br, 32H, Cyclen CH_2), 3.45, 2.44 (br, 16H, Cyclen CH_2), 3.36 (br, 8H, NC*H*COO$^-$), 3.25, 3.14 (br, 16H, NCH_2CH_2), 3.07, 2.81 (br, 16H, Cyclen CH_2), 2.84, 2.73 (br, 16H, Cyclen CH_2), 2.77 (br, 32H, Cyclen CH_2),

(30) Corsi, D. M.; Platas-Iglesias, C.; van Bekkum, H.; Peters, J. A. *Magn. Reson. Chem.* **2001**, 723–726.
(31) Barge, A.; Cravotto, G.; Gianolio, E.; Fedeli, F. *Contrast Med. Mol. Imaging* **2006**, *1*, 184–188.

2.67 (br, 16H, Cyclen), 2.63, 2.35 (br, 16H, CH_2CON), 2.04, 1.88 (br, 16H, $CHCH_2$), 1.64 (br, 16H, CH_2CH_2Si), 0.75 (br, 16H, CH_2Si). $^{13}C\{^1H\}$ NMR (125.76 MHz, D_2O): δ = 180.7, 180.5, 180.3 (COO^-), 175.4 (CON), 68.4 ($NCHCOO^-$), 65.9, 65.8 (br, CH_2COO^-) 56.1, 55.9, 55.6, 55.4, 55.1, 54.7, 54.4, 45.8 (br, Cyclen CH_2), 41.6 (NCH_2CH_2), 34.8 (CH_2CON), 22.0 (CH_2CH_2Si), 20.4 ($CHCH_2$), 8.4 (CH_2Si). $^{29}Si\{^1H\}$ NMR (99.36 MHz, D_2O): δ = −65.3. HRMS (FTICR): $[M]^{8-}$ calcd: 653.48706, found: 653.48702.

NMR characterization data of the yttrium complex of **GB**: ^1H NMR (500.13 MHz, D_2O): δ = 7.77 (m, A-portion of an $[AB]_2$-system, 16H, Ar-2-H, Ar-6-H), 7.37 (br m, B-portion of an $[AB]_2$-system, 16H, Ar-3-H, Ar-5-H), 4.70 (br s, 8H, $CHCOO^-$), 3.79 (br, 8H, $CHHCOO^-$), 3.31 (br, 8H, $CHHCOO^-$), 3.69 (br, 8H, $CHHCOO^-$), 3.31 (br, 8H, $CHHCOO^-$), 3.66 (br, 8H, $CHHCOO^-$), 3.28 (br, 8H, $CHHCOO^-$), 3.29, 2.63 (br, 16H, Cyclen CH_2), 3.29, 2.35 (br, 16H, Cyclen CH_2), 3.29, 2.06 (br, 16H, Cyclen CH_2), 3.22 (br, 16H, NCH_2CH_2), 2.94, 2.75 (br, 16H, Cyclen CH_2), 2.94, 2.37 (br, 16H, Cyclen CH_2), 2.83, 2.21 (br, 16H, Cyclen CH_2), 2.81, 2.47 (br, 16H, Cyclen CH_2), 2.79 (br, 16H, Cyclen CH_2), 1.71 (br, 16H, CH_2CH_2Si), 0.76 (br, 16H, CH_2Si). $^{13}C\{^1H\}$ NMR (125.76 MHz, D_2O): δ = 180.8 (br, CH_2COO^-), 178.3 (br, $CHCOO^-$), 168.8 (br, $ArCON$), 135.3 (br, Ar-4-C), 133.9 (br, Ar-1-C), 132.7 (br, Ar-3-C, Ar-5-C), 126.8 (br, Ar-2-C, Ar-6-C), 74.1 (br, $CHCOO^-$), 66.0 (br, CH_2COO^-), 56.0, 55.9, 55.4, 55.2, 55.0, 54.7, 45.7 (br, Cyclen CH_2) 41.7 (NCH_2CH_2), 22.2 (CH_2CH_2Si), 8.4 (CH_2Si). $^{29}Si\{^1H\}$ NMR (99.36 MHz, D_2O): δ = −65.4. HRMS data of the gadolinium complex of **GB**: HRMS (FTICR): $[M]^{8-}$ calcd: 769.880308, found: 769.881065.

General Procedure for the Synthesis of the Ln-Complexes of the Monomers. Ligand **2** or **3** was dissolved in distilled water (0.5 mL) and a stock solution of $LnCl_3$ (1.1 equiv for YCl_3 and 0.9 equiv for $GdCl_3$) was added. The pH was adjusted to 6−7 using a 1 M solution of NaOH. The mixture was heated to 70 °C for 1 h. After cooling to room temperature, the pH was adjusted to 7.0 using a 1 M solution of NaOH, followed by the evaporation of the solvent. The absence of non-coordinated Gd^{3+} ions in the gadolinium complexes was confirmed by the xylenol test.[31]

PGSE Diffusion ^1H NMR Experiments. PGSE diffusion ^1H NMR measurements were performed by using the standard Bruker stimulated echo pulse sequence on a Bruker Avance II^+ 500 MHz spectrometer equipped with a gradient unit and a multinuclear inverse probe with a Z-gradient coil. The temperature was 298 K, and the sample was not spun. Rectangular gradient pulses with durations (δ) of 1.5 and 1.6 ms for the monomers and 2.4 and 3.0 ms for the Gadoxanes were applied. Their strength (G) was varied during the experiments. The delay between the midpoints of the gradients (Δ) was set to 150 ms for the monomers and 200 ms for the Gadoxanes. The spectra were recorded using 32 to 256 scans, 32K points, a relaxation delay of 1.6−3.5 s, a spectral width of 7500 Hz and were processed with a line broadening of 2 Hz. The intensities of the ^1H resonance of the following moieties were determined in each spectrum: $CHCH_2$ for Y-DOTAGA, Ar-2-H, and Ar-6-H for Y-DOTA-BA, CH_2Si for the Gadoxanes. The plots of $\ln(I/I_0)$ versus G^2 were fitted using a linear regression algorithm to obtain the D values according to eq 1:

$$\ln \frac{I}{I_0} = -(\gamma\delta)^2 D\left(\Delta - \frac{\delta}{3}\right)G^2 \qquad (1)$$

Where I = intensity of the observed spin−echo, I_0 = intensity of the spin−echo without gradients, γ = magnetogyric ratio, δ = length of the gradient pulse, D = diffusion coefficient, Δ = delay between the midpoints of the gradients, and G = gradient strength.

Relaxivity Measurements. Relaxivity measurements during the degradation of **GG** were performed at room temperature (~21 °C) in a 3 T (123 MHz) human MR scanner (MAGNETOM Tim Trio, Siemens Healthcare, Germany), using a 12-channel RF Head coil and slice selective measurements from a slice with a thickness of 1 mm positioned through the samples. The samples (0.8 mL) were freshly prepared for each time point (0−200 h) by making dilutions of **GG** at 0, 12.5, 25, 37.5, and 50 μM gadolinium(III) (1.56, 3.12, 4.69, and 6.25 μM GG) in culture medium (Dulbeccós modified Earlés medium, ± FCS, ± HEPES) in tubes and incubating them at 37 °C and 10% CO_2 with or without gas exchange. The samples were then split into two 0.65 mL tubes prior to the MR relaxivity measurements. The pH of the solutions was determined after the MR measurements. Solutions containing HEPES buffer had a pH in the range of 7.4−7.6 whereas the samples without HEPES and no gas exchange during the incubation period had pH values between 8.1 and 8.6. T_1 was measured using an inversion−recovery sequence, with an adiabatic inversion pulse followed by a turbo-spin−echo readout. Between 10 and 15 images were taken, with the time between inversion and readout varying from 23 to 3000 ms. With a repetition time of 10 s, 15 echoes were acquired per scan and averaged six times. All experiments scanned 256^2 voxels in a field-of-view of 110 mm in both directions resulting in a voxel volume of 0.43 × 0.43 × 1 mm^3. Data analysis was performed by fitting to relaxation curves with self-written routines under MATLAB 7.1 R14 (The Mathworks Inc., U.S.). The series of T_1 relaxation data were fitted according to eq 2 with varying $t = T_I$:

$$S = S_0(1 - e^{-t/T_1}) + S_{T_1=0}(e^{-t/T_1}) \qquad (2)$$

Nonlinear least-squares fitting of three parameters S_0, $S_{(TI=0)}$, and T_1 was done for manually selected regions-of-interest with the Trust-Region Reflective Newton algorithm implemented in MATLAB. The quality of the fit was controlled by visual inspection and by calculating the mean errors and residuals. The r_1 values were plotted versus the incubation time and fitted by a first order exponential decay function to get the degradation kinetics of **GG**. In case of the incubation at higher pH, a fit assuming a second order decay gives a better result indicating a very fast initial degradation of the silsequioxane core at pH > 8.

The degradation of the silsesquioxane core of **GB** was studied by measuring the longitudinal relaxation rates ($1/T_1$) of water protons of an aqueous solution of **GB** ($c(Gd^{3+})$ = 1.99 mM, pH 7.4 (HEPES buffer)) on a Stelar SMARtracer Fast Field Cycling NMR relaxometer at 10 MHz and 37 °C after different periods of time. During the first 36 h the sample was kept in the relaxometer, then the sample was kept in a water bath (37 °C) between the measurements. The r_1 values were plotted versus the time and fitted by a first order exponential decay function using ORIGIN (Microcal, U.S.A.). The reported errors correspond to one standard deviation obtained by the statistical analysis.

^{17}O NMR and NMRD Measurements. The longitudinal and transverse ^{17}O relaxation rates ($1/T_{1,2}$) and the chemical shifts were measured in aqueous solutions of the Gd^{3+} complexes in the temperature range of 275−361 K for the monomers and 275−320 K for the Gadoxanes, on a Bruker Avance II 300 MHz (7.05 T, 40.69 MHz) spectrometer. The Gd^{3+} concentration of the samples was between 9.9 and 16.6 mM, and the pH of the solutions was 6.7 (HEPES buffer). To improve the sensitivity in ^{17}O NMR, ^{17}O-enriched water (10% $H_2{}^{17}O$, CortecNet) was added to the solutions to yield about 3% ^{17}O enrichment. The exact Gd^{3+} concentration was determined using the BMS method.[30] The temperature was determined with ethylene glycol.[32] An acidified water solution was used as reference ($HClO_4$, pH 3.0). The samples were sealed in glass spheres fitted

(32) Ammann, C.; Meier, P.; Merbach, A. *J. Magn. Reson.* **1982**, *46*, 319–321.

into 10 mm NMR tubes to eliminate susceptibility corrections to the chemical shifts.[33] Longitudinal ^{17}O relaxation times (T_1) were measured by the inversion−recovery pulse sequence, and the transverse relaxation times (T_2) were obtained by the Carr−Purcell−Meiboom−Gill spin−echo technique.

Proton NMRD profiles were recorded on a Stelar SMARtracer Fast Field Cycling NMR relaxometer (0.01−10 MHz) and a Bruker WP80 NMR electromagnet (20, 40, 60, and 80 MHz) adapted to variable field measurements and controlled by the SMARtracer PC-NMR console. The temperature was controlled by a VTC91 temperature control unit and maintained by a gas flow. The temperature was determined according to previous calibration with a Pt resistance temperature probe. The relaxivities at 250, 400, and 500 MHz were measured on a Bruker DRX 250 MHz, a Bruker Avance II 400 MHz, and a Bruker Avance II$^+$ 500 MHz spectrometer, respectively. The temperature was determined with ethylene glycol.[32] The least-squares fits of the ^{17}O NMR and ^1H NMRD data were performed by using Micromath Scientist version 2.0 (Salt Lake City, UT, U.S.A.). The reported errors correspond to one standard deviation obtained by the statistical analysis.

Results and Discussion

Synthesis of the Ligands. The most common macrocyclic ligand for lanthanide complexation is 1,4,7,10-tetraazacyclododecane-1,4,7,10-tetraacetic acid (H_4DOTA, **1**, Figure 2). To bind DOTA to other molecules without lowering the complex stability and water exchange rate, an additional functional group is required. A relatively convenient way is the functionalization of the methylene group of one of the acetate pendant arms with an additional carboxylic acid. Furthermore, it has been shown that it is possible to directly couple the functionalized monohydrated gadolinium complex to a designated molecule without using protecting groups, as the four DOTA-carboxylate groups are protected by the coordination to the gadolinium(III) ion.[13]

For the synthesis of Gadoxane G (**GG**) a new route to the known ligand 1,4,7,10-tetraazacyclododecane-1-glutaric-4,7,10-triacetic acid (H_5DOTAGA, **2**, Figure 2)[34] was used. To synthesize Gadoxane B (**GB**), the novel ligand 1,4,7,10-tetraazacyclododecane-1-(4-(carboxymethyl)-benzoic)-4,7,10-triacetic acid (H_5DOTABA, **3**, Figure 2) was developed.

The synthetic strategy for both ligands implies the alkylation of the secondary nitrogen of tri-*tert*-butyl 1,4,7,10-tetraazacyclododecane-1,4,7-triacetate (DO3A(^{t}Bu)$_3$, **10**, Scheme 3) by an appropriate protected 2-bromodicarboxylic acid. Dimethyl 2-bromoglutarate (**5**) for the synthesis of DOTAGA was obtained in a two-step procedure (Scheme 1). Glutamic acid (**4**) was converted into 2-bromoglutaric acid via diazotation analogous to the method described by Holmberg.[35] The crude acid, being about 85% pure by NMR spectroscopy, was then directly treated with methanol in the presence of conc. sulfuric acid to afford the desired protected product **5** in 75% yield.

For the synthesis of DOTABA, methyl 4-((methoxycarbonyl)bromomethyl)benzoate (**9**) was prepared in three steps from the commercially available methyl 4-(cyanomethyl)-benzoate (**6**) (Scheme 2). Following the literature procedure[29] **6** was hydrolyzed to afford 4-(carboxymethyl)-benzoic acid (**7**) in 84% yield. Protection of the acid groups using thionyl chloride in methanol gave the dimethyl ester (**8**) in 95% yield.

The bottleneck of this route was the bromination of **8**. When **8** was refluxed with *N*-bromosuccinimide (NBS) and catalytic amounts of azobisisobutyronitrile (AIBN) in carbon tetrachloride for 5 h the conversion was only about 49% according to ^1H NMR spectroscopy. Readdition of AIBN and additional 17 h heating to reflux were necessary to achieve at least 73% conversion. As a complete separation of **9** from unreacted **8** by column chromatography proved unsuccessful, **9** could be obtained in only 48% yield. Interestingly, a much poorer conversion was achieved if the initial reaction time was prolonged to 24 h.

DO3A(^{t}Bu)$_3$ (**10**) was then treated with the two obtained dimethyl 2-bromodicarboxylates **5** or **9** in the presence of a base, to afford **11** and **12** as the protected forms of DOTAGA and DOTABA, respectively (Scheme 3). The successful synthesis of **11** and **12** in 71% and 86% yield, respectively, was confirmed by two-dimensional ^1H and ^{13}C NMR spectroscopy and high resolution mass spectrometry (HR-MS). The lower yield of **11** as compared to **12** might be explained by the possible HBr elimination as a side reaction. Complete deprotection of

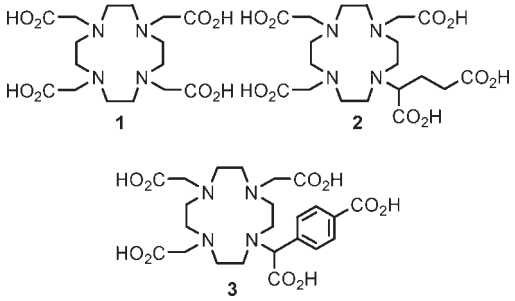

Figure 2. Structures of the ligands H_4DOTA (**1**), H_5DOTAGA (**2**), and H_5DOTABA (**3**).

Scheme 1. Synthesis of Dimethyl 2-Bromoglutarate (**5**)

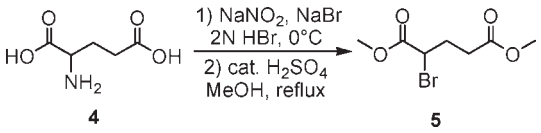

Scheme 2. Synthesis of Methyl 4-((Methoxycarbonyl)bromomethyl)-benzoate (**9**)

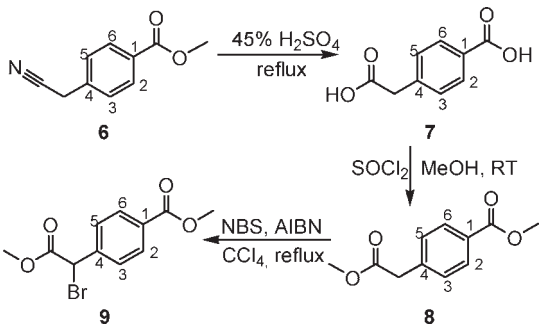

(33) Hugi, A. D.; Helm, L.; Merbach, A. E. *Helv. Chim. Acta* **1985**, *68*, 508–521.
(34) Eisenwiener, K.-P.; Powell, P.; Macke, H. R. *Bioorg. Med. Chem. Lett.* **2000**, *10*, 2133–2135.
(35) Holmberg, B. *Chem. Ber.* **1927**, *60*, 2198–2211.

Scheme 3. Synthesis of H_5DOTAGA (**2**) and H_5DOTABA (**3**)

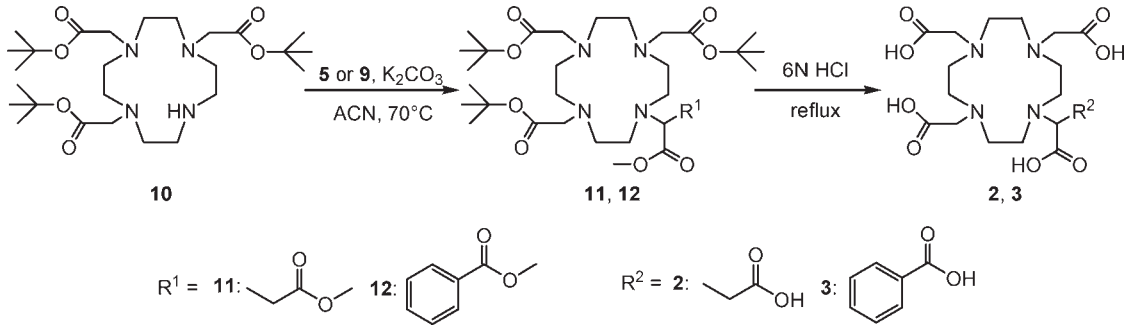

Scheme 4. Complexation Reactions of H_5DOTAGA (**2**) and H_5DOTABA (**3**)

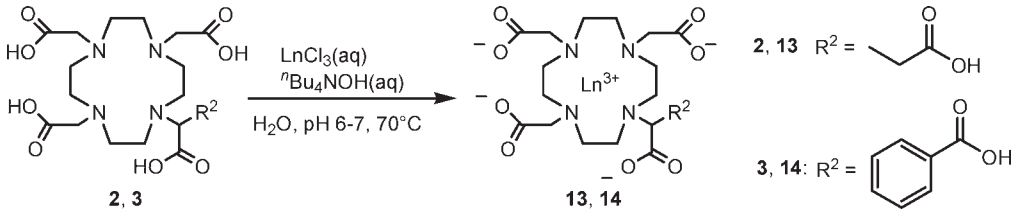

Scheme 5. Synthesis of Gadoxane G (**GG**) and Gadoxane B (**GB**)

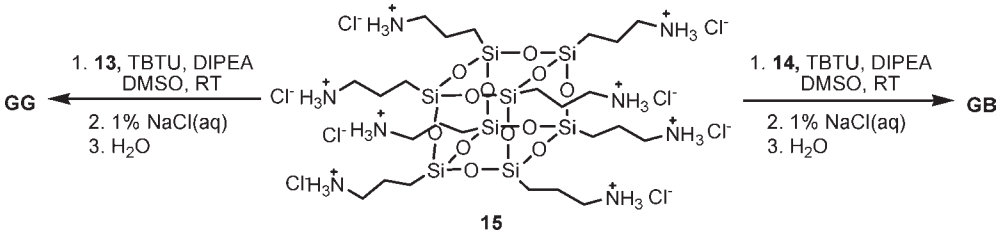

the ligands was achieved in excellent yields by refluxing their aqueous 6 N hydrochloric acid solutions overnight. The ligands **2** and **3** were obtained as their ammonium chloride salts. Rough titrations of the products at about pH 6 with a YCl_3 solution and xylenol orange as the indicator yielded the equivalence point after the addition of about 0.85 equiv of Y(III) referred to the respective molecular masses of the uncharged structure of **2** and **3** as shown in Figure 1. This would correspond to about 2.5 to 3 HCl molecules per ligand. However, as the product is slightly hygroscopic, some water can also contribute to the increased molecular mass. Organic impurities are not responsible as the ^{1}H and ^{13}C NMR spectra in D_2O contained only signals of the desired product. The yield of complexing species was calculated to be about 92% and 90% for **2** and **3**, respectively.

All steps were characterized by ^{1}H and $^{13}C\{^1H\}$ NMR spectroscopy and HR-MS, if procurable. The purity of dimethyl 2-bromoglutaric acid (**5**) and methyl 4-((methoxycarbonyl)bromomethyl)benzoate (**9**) was additionally demonstrated by elemental analysis.

Synthesis of Gadoxane G and B. The lanthanide complexes **13** and **14** were prepared by treating aqueous solutions of **2** and **3**, respectively, with aqueous solutions of $LnCl_3$ (Ln = Gd^{3+}, Y^{3+}) while adjusting the pH to 6−7 using hydroxide as base (Scheme 4). To increase the solubility of the negatively charged complexes in nonaqueous solvents as required for the following grafting to the silsesquioxane, tetra-*n*-butylammonium hydroxide was used in these cases. (In the preparation of the monomer complexes, tetra-*n*-butylammonium hydroxide was replaced by sodium hydroxide.) Complete complexation was achieved by stirring the solutions for several hours at increased temperature. The solvent of the respective reaction mixture was then removed under reduced pressure, and the residue was kept in vacuo for 4 to 6 days to remove most of the remaining water. It should be noted that the solubility of the ^{n}Bu$_4$N[Ln(DOTABA)H_2O] (Ln = Gd^{3+}, Y^{3+}) complexes in water is extremely low leading to a white precipitate once the complex has been formed. With sodium as the counterion the solubility of **14** is significantly higher, but still low compared to **13**.

The covalent binding of **13** and **14** to octa(3-chloroammoniumpropyl)silsesquioxane (**15**) was achieved by treating the silsesquioxane and an excess of the respective complex with *O*-(benzotriazol-1-yl)-*N*,*N*,*N*′,*N*′-tetramethyluronium tetrafluoroborate (TBTU) and *N*,*N*-diisopropylethylamine (DIPEA) in dimethyl sulfoxide (DMSO) (Scheme 5).

The tetra-*n*-butylammonium salt of **13** is fairly soluble in DMSO; however, the process is relatively slow. Once **13** is dissolved, the coupling to the silsesquioxane is achieved quantitatively within several minutes. For the tetra-*n*-butylammonium salt of **14** the solubility in DMSO is significantly lower. Since therefore the synthesis had to be carried out in suspension, the reaction time was increased to 3 h.

In both cases the reaction was quenched by adding the reaction mixtures to a diluted acetic acid/sodium acetate

Table 1. Translational Diffusion Coefficient D and Resultant Hydrodynamic Radius r_H, Hydrodynamic Volume V_H, and Rotational Correlation Time τ_{RDiff} at 25 °C of **GG**, **GB**, Y-DOTAGA (**13**), and Y-DOTABA (**14**)

compound	D [m^2/s]	r_H [nm]	V_H [nm^3]	τ_{RDiff} [ps]
Gadoxane G (**GG**)	$(1.373 \pm 0.008) \times 10^{-10}$	1.442 ± 0.008	12.56 ± 0.22	3370 ± 60
Gadoxane B (**GB**)	$(1.379 \pm 0.007) \times 10^{-10}$	1.436 ± 0.007	12.40 ± 0.19	3320 ± 50
Y-DOTAGA (**13**)	$(3.976 \pm 0.009) \times 10^{-10}$	0.499 ± 0.001	0.52 ± 0.00	139 ± 1
Y-DOTABA (**14**)	$(3.625 \pm 0.008) \times 10^{-10}$	0.547 ± 0.001	0.68 ± 0.01	183 ± 1

buffer (pH 5.5). Purification of the Gadoxanes was achieved via diafiltration using a membrane with a molecular weight cutoff of 3K. During the filtration process the tetra-*n*-butylammonium counterion was fully replaced by sodium to afford **GG** and **GB** as their octasodium salts in about 37% and 30% yield, respectively. As the obtained colorless solids might contain residual sodium chloride, the yield was determined by measuring the gadolinium(III) concentrations in known volumes using the BMS method.[30] The yield can be improved by using a smaller cutoff; however, this happens at the expense of purity.

Compounds **GG** and **GB** were characterized on the basis of their yttrium(III) complexes by multinuclear (^{1}H, ^{13}C, ^{29}Si) NMR spectroscopy. All spectra were measured in D_2O at 25 °C and pD 7.0. The ^{1}H NMR spectra of **GG** and **GB** are given in the Supporting Information. A complete assignment of the ^{1}H and ^{13}C NMR resonances to the structures of **GG** and **GB** was achieved using two-dimensional techniques. Because of the cubic symmetry of the silsesquioxane core, the ^{29}Si NMR spectra show only one ^{29}Si signal at −65.3 ppm and −65.4 ppm for **GG** and **GB**, respectively. Additionally, HR mass spectra of the yttrium(III) complex of **GG** and the gadolinium(III) complex of **GB** were recorded (Supporting Information). No signals corresponding to less than eight-times substituted silsesquioxanes, partly hydrolyzed or free monomeric complexes (**13** or **14**) were detected. Furthermore, no hydrolysis products were observed in samples which were stored at −28 °C for more than 10 months. The absence of non-coordinated lanthanide(III) ions was confirmed by the xylenol test.[31]

PGSE Diffusion NMR. The molecular size is an important parameter for a CA. Not only that the size or rather the related rotational correlation time τ_R is a key factor for the relaxivity of a CA, it also has a significant impact on its distribution within the body and its excretion rate. Over the past years, pulsed-field gradient spin echo (PGSE) diffusion NMR spectroscopy has shown to be a powerful tool in determining the size and also the rotational correlation time of very small to extremely large molecules.[36−38]

Using PGSE diffusion ^{1}H NMR spectroscopy, the translational self-diffusion coefficients D of the yttrium complexes of **GG** and **GB** as well as of the two monomers (**13** and **14**) were determined at 25 °C. For spherical molecules, like the Gadoxanes and in good approximation also the monomers, D is related to the hydrodynamic radius r_H via the Stokes−Einstein equation (eq 3):

$$D = \frac{k_B T}{6\pi\eta r_H} \tag{3}$$

where k_B is the Boltzmann constant, T the absolute temperature, η the viscosity, and r_H the hydrodynamic radius. The hydrodynamic volume V_H and the rotational correlation time τ_{RDiff} in turn can be calculated from r_H applying eqs 4 and 5, respectively:

$$\tau_{RDiff} = \frac{4\pi\eta r_H^3}{3k_B T} \tag{4}$$

$$V_H = \frac{4}{3}\pi r_H^3 \tag{5}$$

As diluted samples (2−3 mM of the Gadoxanes and 15−20 mM for the monomers) were used, r_H, V_H and τ_{RDiff} could be calculated from the diffusion constants assuming $\eta_{solution} = \eta_{solvent}$ (Table 1).[39]

Evaluation of the diffusion data revealed almost identical hydrodynamic radii for **GG** and **GB** (1.44 nm), showing that the different linkers have no net effect on the size of the CA. By contrast, in the case of the monomers, the use of a phenyl spacer instead of an ethylene spacer leads to a significant increase in the hydrodynamic volume V_H of about 30% (0.52 nm^3 and 0.68 nm^3 for Y-DOTAGA and Y-DOTABA, respectively). With hydrodynamic volumes of 12.56 nm^3 and 12.40 nm^3, the two Gadoxanes are thereby about 20-times larger than their respective monomers. This should result in a significant increase in relaxivity, especially at field strengths currently used in clinical MRI. Furthermore, the Gadoxanes are still considerably smaller than the small pores (3−5 nm) of the glomerular filter in the kidneys,[40,41] which should allow a sufficiently fast clearance of the Gadoxanes from the body.

Stability of the Silsesquioxane Cage in Aqueous Media. Silsesquioxanes are formed in hydrolysis and condensation reactions. Thus, hydrolysis can be an issue in aqueous media. However, as most of the so far reported silsesquioxanes are insoluble in water, not much data are available on their hydrolysis in aqueous media. Feher et al.[42] referred the stability of octa(3-chloroammoniumpropyl)silsesquioxane (**15**) to be very high in neutral or acidic solutions, though no quantitative data were given. On the other hand, they reported the appearance of a prominent new set of resonances in the ^{29}Si NMR spectrum of an alkaline D_2O solution (pH 9) of **15** 10 min after preparation. These resonances, which grow at the expense

(36) Cohen, Y.; Avram, L.; Frish, L. *Angew. Chem., Int. Ed.* **2005**, *44*, 520–554.
(37) Macchioni, A.; Ciancaleoni, G.; Zuccaccia, C.; Zuccaccia, D. *Chem. Soc. Rev.* **2008**, *37*, 479–489.
(38) Yao, S.; Babon, J. J.; Norton, R. S. *Biophys. Chem.* **2008**, *136*, 145–151.
(39) Lewis, G. N.; Macdonald, R. T. *J. Am. Chem. Soc.* **1933**, *55*, 4730–4731.
(40) Booth, J. W.; Lumsden, C. J. *Biophys. J.* **1993**, *64*, 1727–1734.
(41) Tencer, J.; Frick, I.-M.; Oquist, B. W.; Alm, P.; Rippe, B. *Kidney Int.* **1998**, *53*, 709–715.
(42) Feher, F. J.; Wyndham, K. D.; D., S.; F., N. *Dalton Trans.* **1999**, 1491–1497.

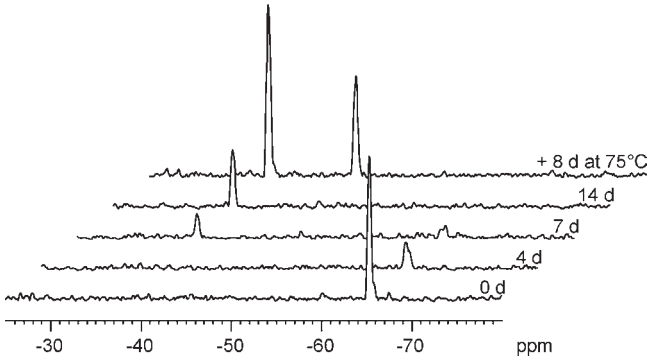

Figure 3. ^{29}Si projections of ^{1}H−^{29}Si HSQC NMR spectra of the yttrium(III) complex of **GG** after 0 d, 4 d, 7 d, 14 d at 25 °C (pD 7.0), and after additional 8 days at 75 °C.

of the resonance for **15**, are believed to belong to a silsesquioxane cage, in which one Si−O−Si bond is cleaved. Attempts to achieve higher conversion then led to complete decomposition of the cage.

To investigate the stability of the silsesquioxane cage of the Gadoxanes toward hydrolysis, ^{29}Si NMR spectra of an aqueous solution (pD 7.0) of the yttrium(III) complex of Gadoxane G (**GG**) were measured at 25 °C as a function of time. To reduce the acquisition time, the ^{29}Si NMR spectra were recorded via a 2D ^{1}H−^{29}Si HSQC experiment (Figure 3). The spectrum measured directly after preparation of the solution shows only one signal in the typical range of T^3 groups[43] at −65.3 ppm (trace 0 d). The solution was then kept at 25 °C for 2 weeks during which further ^{1}H−^{29}Si HSQC NMR spectra were recorded (Figure 3). The intensity of the resonance at −65.3 ppm slowly decreased during this period of time, clearly indicating the hydrolysis of the silsesquioxane. This leads to various T^n (n = 1−3) species with much lower symmetry which generate numerous magnetically inequivalent ^{29}Si nuclei in poor concentrations circumventing their detection in a reasonable time.

After 7 days, a new signal appeared at −38.2 ppm which is in the range of T^0 groups[44] and thus is assigned to the fully hydrolyzed species **17** (Scheme 6). After 14 days, the intensity of this peak had further increased, and a very small signal at −47.9 ppm could also be observed. As this resonance is in the range for T^1 groups, it is assigned to the $(OH)_2RSi$-O-$SiR(OH)_2$ fragment (**18**) (Scheme 6).

To achieve complete hydrolysis, after 14 days at 25 °C, the solution was heated to 75 °C. In a spectrum measured after 2 days the signal due to **18** had not vanished, but on the contrary, the intensities of both **17** and **18** strongly increased. The ratio between them remained unchanged even after the solution was kept at 75 °C for additional 6 days, suggesting an equilibrium between the two species, **17** and **18**.

Simultaneously to the ^{29}Si NMR measurements, the same solution was also used to determine the translational self-diffusion coefficient D of Gadoxane G (**GG**) and of its fragments by PGSE diffusion ^{1}H NMR spectroscopy at 25 °C (Figure 4). All fragments are measured

Scheme 6

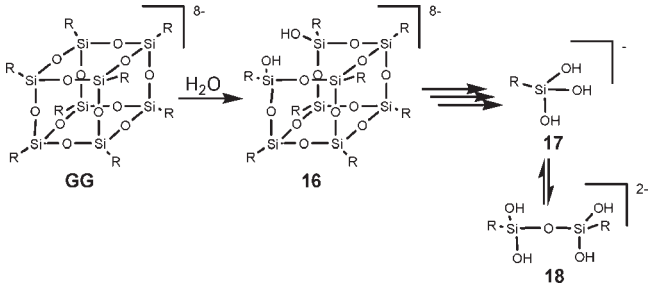

Table 2. Translational Diffusion Coefficient D, Hydrodynamic Radius r_H, Hydrodynamic Volume V_H, and Rotational Correlation Time τ_R at 25 °C of Gadoxane G (**GG**) (time = 0), Y-DOTAGA (**13**), and the Average Values during the Decomposition of **GG**

time [d]	D [m^2/s]	r_H [nm]	V_H [nm^3]	τ_R [ps]
0 (**GG**)	1.37×10^{-10}	1.44	12.56	3366
0.375	1.39×10^{-10}	1.42	12.00	3216
1	1.43×10^{-10}	1.38	11.05	2960
2	1.43×10^{-10}	1.39	11.14	2985
3	1.48×10^{-10}	1.34	10.01	2682
4	1.47×10^{-10}	1.34	10.17	2726
5	1.51×10^{-10}	1.32	9.54	2555
7	1.54×10^{-10}	1.28	8.83	2367
14	1.64×10^{-10}	1.21	7.38	1979
+ 8d at 75 °C	2.63×10^{-10}	0.75	1.78	477
Y-DOTAGA (**13**)	3.98×10^{-10}	0.50	0.52	139

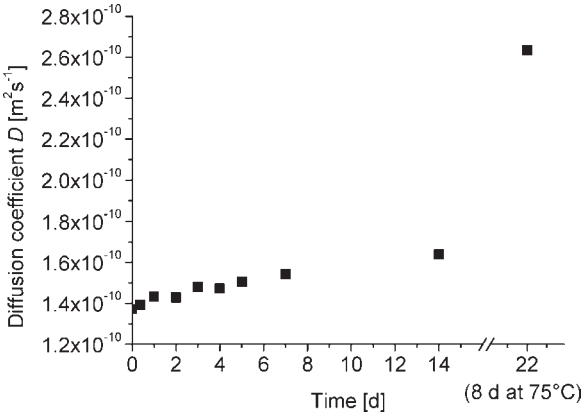

Figure 4. Average translational diffusion coefficient D of Gadoxane G (**GG**) and its fragments at 25 °C (pD 7.0) as a function of time.

with the same sensitivity than the undamaged species which makes PGSE NMR ideal for following decomposition processes. However, as the signals of **GG** and its fragments could not be separated in the ^{1}H NMR spectra, only an average diffusion coefficient of all species was obtained during the decomposition of **GG**.

The sample was diluted (the initial concentration of Gadoxane was about 2−3 mM), therefore r_H, V_H, and τ_R were again calculated from the diffusion constants assuming $\eta_{solution} = \eta_{solvent}$ (Table 2).[39]

For comparison, the data of Y-DOTAGA (**13**) is also included in the table. As already reported above, 1.37×10^{-10} m^2 s^{-1} was obtained for the diffusion coefficient of the undamaged **GG** (time = 0). The average diffusion coefficient of **GG** and its fragments then slowly increased with time (Figure 4 and Table 2). As not all fragments are supposed to be spherical, the Stokes−Einstein equation is

(43) Lindner, E.; Schneller, T.; Auer, F.; Mayer, H. A. *Angew. Chem., Int. Ed.* **1999**, *38*, 2154–2174.
(44) Sugahara, Y.; Inouea, T.; Kuroda, K. *J. Mater. Chem.* **1997**, *7*, 53–59.

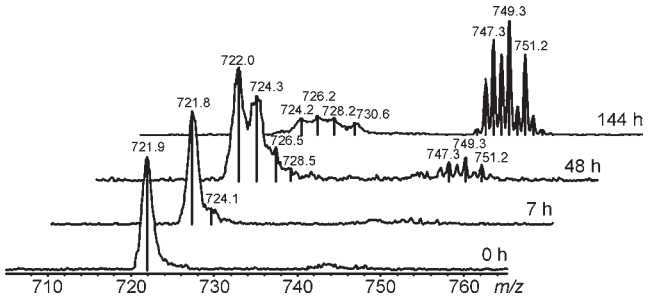

Figure 5. ESI mass spectra of the gadolinium(III) complex of Gadoxane G (**GG**) and its fragments after 0, 7, 48, and 144 h at 37 °C and pH 7.0.

in this case not generally valid and therefore the resulting average values of r_H, V_H, and τ_R during decomposition (Table 2) can only be considered as approximations. It is still conspicuous that after 14 days the average V_H had only decreased to about half the value of the undamaged Gadoxane. Although the corresponding ^{29}Si NMR spectrum displayed no resonances due to T^3 and T^2 groups after that time, this points out that a considerable amount of only partly degraded species still remains under these conditions. Heating the solution to 75 °C for additional 8 days then changed D significantly, showing that higher temperatures are necessary to obtain mostly small fragments at neutral pH within a reasonable time.

A possibility to follow the single steps of the hydrolysis in more detail is offered by electrospray ionization mass spectrometry (ESI-MS). The gadolinium(III) complex of Gadoxane G (**GG**) was used for this investigation. As the reaction rate increases with temperature, the aqueous solution of **GG** was kept at 37 °C and pH 7.0. ESI mass spectra were recorded at the outset, after 7, 48, and 144 h (Figure 5). With a molar mass of 5774.95 g/mol, the eight-times negatively charged gadolinium complex has a m/z of 721.9. Unlike in the high resolution mass spectra, the isotopic pattern of this highly charged compound could not be resolved in these ESI mass spectra. Instead a broad signal appeared in the starting spectrum. Each breaking of a Si−O−Si moiety involves the addition of a water molecule (Scheme 6). For an eight-times negatively charged compound this corresponds to an increase in m/z of 2.25. The hydrolysis of the first Si−O−Si unit was observed after 7 h by the appearance of the signal at m/z = 724.1. After 48 h, the spectrum showed additional signals corresponding to two and three hydrolyzed Si−O−Si moieties in the silsesquioxane core. Moreover the isotope pattern of the fully degraded species **17** at m/z = 749.3 begins to grow in. The signal corresponding to the undamaged species had almost vanished when the solution was kept for additional 96 h, whereas the isotope pattern of **17** was now clearly visible. Interestingly no signals corresponding to seven- to two-times negatively charged fragments could be observed by this method.

The degradation rate of Gadoxane G (**GG**) under physiological conditions was tested via relaxivity measurements. Various concentrated solutions of the gadolinium(III) complex of **GG** in typical cell culture media (20 mM HEPES, pH 7.4−7.6) with and without fetal calf serum (FCS) were incubated at 37 °C, for different periods of time. T_1-relaxation times of the solutions were measured at 3 T and room temperature. No significant

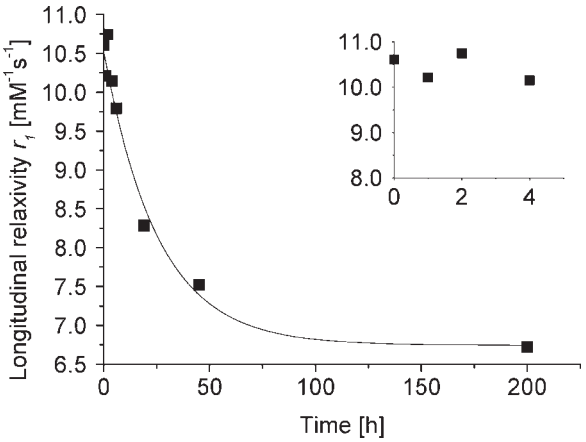

Figure 6. Longitudinal relaxivity r_1 (3 T, r.t.) during the degradation of **GG** under physiological conditions (cell culture media, 20 mM HEPES, pH 7.4−7.6). The inset highlights the first 4 h of incubation.

differences between the serum containing and serum free solutions could be observed. Thus, for the further evaluations, the data of both experiments were combined. The respective longitudinal relaxivities r_1 were calculated from the T_1 measurements (Figure 6). Without incubation, a longitudinal relaxivity of 10.6 mM^{-1} s^{-1} per gadolinium(III) ion was obtained. Within the first 3 to 4 h of incubation r_1 did not significantly change. This is understandable as the gadolinium(III) ion remains complexed safely, and the initial breaking of Si−O−Si moieties does not have much influence on the size (Scheme 6) and thus on the rotational correlation time τ_R. Further hydrolysis then leads to smaller fragments with a reduced average τ_R resulting in a decrease of r_1. Fitting the period of decrease with a first order exponential decay showed a half-life $t_{1/2}$ of about 15 ± 3 h. A plateau of 6.7 mM^{-1} s^{-1} is reached after about 125 h. This relaxivity still belongs to an equilibrium between the fully hydrolyzed **17** and fragment **18** (Scheme 6).

When the same measurements were performed in solutions of pH 8.1 to 8.6 (without HEPES and gas exchange) the decay was much faster ($t_{1/2}$ about 55 min), and, even more important, the plateau was significantly lower (5.4 mM^{-1} s^{-1}) showing that the increase in pH can further shift the equilibrium toward **17**. The degradation of the silsesquioxane core of Gadoxane B (**GB**) was also investigated by its effect on the longitudinal relaxivity r_1. Since the water itself (or rather OH^-) is responsible for the degradation of the silsesquioxane and no influence of serum, but a strong dependency on the pH was observed for **GG**, the measurements were carried out in HEPES buffered water (pH 7.4), where the pH can be adjusted more accurately. The sample was kept at 37 °C, and the longitudinal relaxation time T_1 was measured at a proton Larmor frequency of 10 MHz after different periods of time. The longitudinal relaxivities were calculated from these data (Figure 7). As was observed for **GG**, r_1 of **GB** also remained constant (14.14 ± 0.08 mM^{-1} s^{-1}) within the first 3 h and only then started to decrease. This decrease could also be fitted with a first order exponential decay. With a half-life $t_{1/2}$ of 11.2 ± 0.2 h the decay rate is comparable to that obtained for **GG** ($t_{1/2}$ = 15 ± 3 h).

^{17}O NMR and NMRD Measurements. The diffusion measurements revealed a rotational correlation time

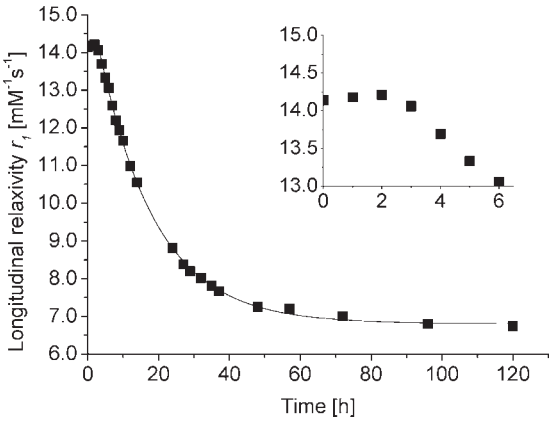

Figure 7. Longitudinal relaxivity r_1 of Gadoxane B (**GB**) under physiological conditions as a function of the time (37 °C, pH 7.4, 10 MHz). The inset highlights the first 6 h of incubation.

τ_{RDiff} of about 3.35 ns for both Gadoxanes (Table 1), which should result in highly efficient CAs. However, τ_{RDiff} reflects the rotational correlation time of the whole molecule, and the relaxivity of a CA is influenced not only by the global rotational tumbling of the compound but also by the local movement of the attached gadolinium-(III) complexes. The difference between the global and the local rotational dynamics is in turn based on the internal flexibility of the macromolecule. Therefore, the introduction of the more rigid phenyl spacer in the linking group of Gadoxane B (**GB**) should result in higher relaxivities for **GB** as compared to Gadoxane G (**GG**) which possesses the more flexible ethylene spacer.

To quantify the effect of the different rigidity of the linking group on the rotational motion of the gadolinium-(III) complexes in **GG** and **GB**, and to determine the parameters describing water exchange and electronic relaxation, variable-temperature ^{17}O NMR and ^{1}H NMRD measurements were performed on aqueous solutions of the gadolinium complexes of **GG** and **GB** as well as of the corresponding monomers Gd-DOTAGA (**13**) and Gd-DOTABA (**14**). For both monomers, the ^{17}O reduced transverse relaxation rates ($1/T_{2r}$) increase at lower temperatures, while above ~300 K they decrease with temperature (slow and fast exchange regions, respectively; Figures 8 and 9). In the slow exchange region, the reduced transverse relaxation rate is given exclusively by the water exchange rate k_{ex}. In the fast exchange regime, it is defined by the transverse relaxation rate of the bound water oxygen $1/T_{2m}$, which is in turn influenced by k_{ex}, the longitudinal electronic relaxation rate $1/T_{1e}$, and the scalar coupling constant $A/\hbar$. The reduced ^{17}O chemical shifts are determined by $A/\hbar$, and to a small extent by an outer-sphere contribution C_{OS}.

Because of the significantly increased instability of the silsesquioxane core at higher temperatures, the ^{17}O reduced transverse relaxation rates of the Gadoxanes could only be obtained in a temperature range of 273−320 K (see Supporting Information). Nevertheless, even in this limited temperature range, both the slow and fast exchange regimes are observable for Gadoxane G and B evidencing that the water exchange rate k_{ex} on the gadolinium complexes is not significantly changed by the attachment to the silsesquioxane core.

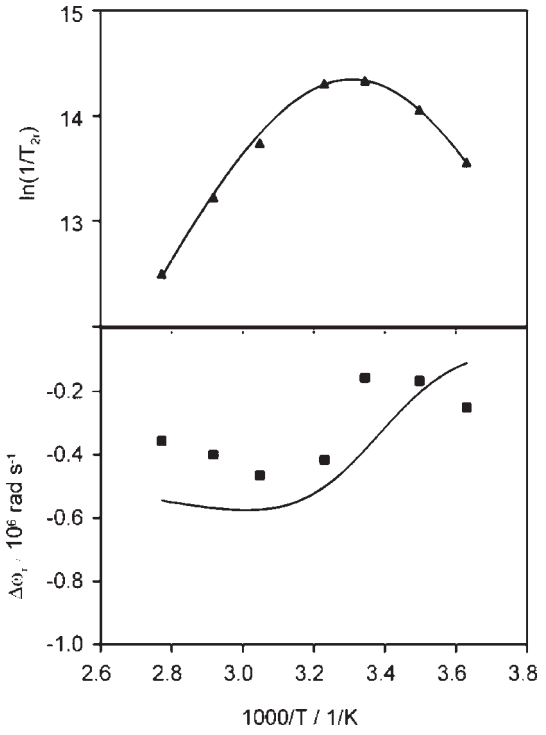

Figure 8. Temperature dependence of the reduced transverse relaxation rates, $1/T_{2r}$, and chemical shifts, $\Delta_{\omega r}$, of Gd-DOTAGA (**13**). B = 7.05 T. The lines represent the least-squares simultaneous fit of all data points.

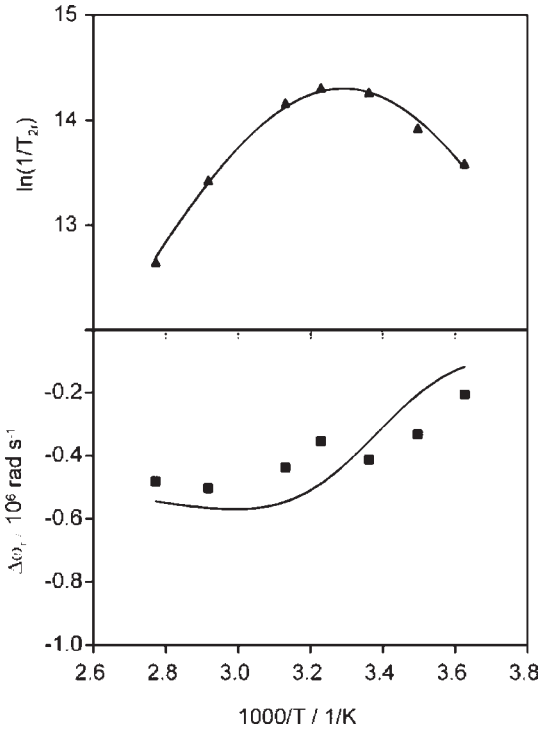

Figure 9. Temperature dependence of the reduced transverse relaxation rates, $1/T_{2r}$, and chemical shifts, $\Delta_{\omega r}$, of Gd-DOTABA (**14**). B = 7.05 T. The lines represent the least-squares simultaneous fit of all data points.

As the transverse ^{17}O relaxation is governed by the scalar relaxation mechanism, it contains no information on the rotational motion of the system. In contrast to $1/T_{2r}$, the longitudinal ^{17}O relaxation rates $1/T_{1r}$ are determined by dipole−dipole and quadrupolar relaxation

Table 3. Parameters Obtained from the Independent Fit of ^{17}O NMR and ^{1}H NMRD Data[a]

	Gd-DOTAGA (**13**)		Gadoxane G (**GG**)		Gd-DOTABA (**14**)		Gadoxane B (**GB**)	
$\Delta H^{\ddagger}$ (kJ mol^{-1})	49.9 ± 0.5		43.5 ± 0.5		47.5 ± 0.5		42.2 ± 0.5	
$\Delta S^{\ddagger}$ (J mol^{-1} k^{-1})	+52 ± 2		+30 ± 2		+43 ± 2		+25 ± 2	
k_{ex}^{298} (10^6 s^{-1})	5.9 ± 0.3		5.3 ± 0.5		5.4 ± 0.3		5.5 ± 0.5	
E_{1H} (kJ mol^{-1})	17.2 ± 0.3[b]		23 ± 0.8		19.7 ± 0.3[b]		20 ± 0.8	
τ_{1H}^{298} (ps)	93 ± 8[b]		240 ± 10		117 ± 10[b]		380 ± 20	
E_{gR} (kJ mol^{-1})			23 ± 0.8				19.3 ± 0.8	
τ_{gR}^{298} (ps)			1500 ± 400				1900 ± 400	
S^2			0.14 ± 0.02				0.21 ± 0.02	
τ_v^{298} (ps)	6.6 ± 0.3	6.5 ± 0.3	3.9 ± 0.4	30 ± 8	9.7 ± 0.7	7.0 ± 0.4	4.5 ± 0.3	31 ± 8
Δ^2 (10^{19} s^{-2})	5.1 ± 0.3	3.9 ± 0.4	5.0 ± 0.4	0.71 ± 0.06	5.0 ± 0.3	3.9 ± 0.4	5.0 ± 0.3	0.62 ± 0.05

[a] For each complex, the left and right semicolumns show the electron spin relaxation parameters calculated from ^{17}O NMR and ^{1}H NMRD, respectively. In the NMRD analysis, the parameters of the water exchange were fixed to values obtained by ^{17}O NMR. [b] No Lipari−Szabo treatment; only a single τ_{RH}^{298} and E_{RH} is calculated

mechanisms, both related to rotation. The dipolar term depends on the Gd^{3+}-water oxygen distance, r_{GdO}, while the quadrupolar term is influenced by the quadrupolar coupling constant, $\chi(1 + \eta^2/3)^{1/2}$. The longitudinal relaxation rates have been also measured; however, the differences between the diamagnetic reference and the paramagnetic samples were too small because of the low Gd^{3+} concentration because of the poor solubility of the complexes, in particular of **14**. Therefore, the reduced longitudinal ^{17}O relaxation rates have not been included in the analysis. The relatively bad accuracy of the chemical shift measurements under these circumstances should also be noted. Nevertheless, in accordance to related systems, the shifts confirm the hydration number of one for all four compounds.

In recent years, it has become general practice to fit ^{17}O NMR and NMRD data simultaneously, which is thought to yield more physically meaningful parameters.[45] However, such an approach was not possible in the case of both Gadoxanes, as an acceptable fit of the ^{1}H relaxation profile could not be reconciled with the electronic relaxation parameters obtained from the ^{17}O NMR studies. This discrepancy is most probably related to an inadequate description of the electron spin relaxation, having a strong influence on both the low-field proton relaxivities and the transverse ^{17}O relaxation rates in the intermediate and fast water exchange regimes. A new appropriate theory that is capable of describing the field dependence (low frequency part of the NMRD curve: < 0.02 T; ^{17}O data: 7.05 T) of electron spin relaxation rates by the inclusion of both transient and static zero-field splitting (ZFS) has been reported.[46,47] However, this theory is only applicable to small molecular weight chelates and not to larger compounds like **GG** and **GB**. Indeed, attempts to simultaneously fit ^{17}O T_2 and NMRD data failed in the case of the "intermediate" size metallostar compound as well.[25]

Therefore, for all four compounds, the transverse ^{17}O relaxation rates, which give access first of all to the water-exchange rate, were fitted together with the ^{17}O chemical shifts using the traditional Solomon−Bloembergen−Morgan equations (see Supporting Information). From these fittings the water exchange rate k_{ex}^{298}, its activation entropy $\Delta S^{\ddagger}$, and enthalpy $\Delta H^{\ddagger}$, as well as the parameters of the electron spin relaxation, namely, the correlation time for the modulation of the zero-field-splitting τ_v^{298} and the mean-square zero-field-splitting energy Δ^2 have been adjusted. In the fit, the scalar coupling constant $A/\hbar$, was fixed to -3.6×10^6 rad s^{-1}. The empirical constant describing the outer sphere contribution to the ^{17}O chemical shift, C_{os}, was set to 0.1, and the activation energy of the correlation time for the modulation of the zero-field-splitting, E_v, was fixed to 1 kJ mol^{-1}. The values obtained for the other parameters are presented in Table 3. The water exchange rates of all four compounds are higher than that reported for Gd-DOTA ($k_{ex}^{298} = (4.1 \pm 0.2) \times 10^6$ s^{-1}).[45] **13** shows the strongest increase in k_{ex}^{298} as compared to Gd-DOTA (about 40%). The large activation enthalpies, $\Delta H^{\ddagger}$, and the positive activation entropies, $\Delta S^{\ddagger}$, suggest a dissociative mechanism for all compounds.[48] In such a dissociative mechanism, the additional negatively charged carboxyl group in **13**, being relatively close to the coordination cage, can favor the leaving of the coordinated water molecule, thus resulting in faster exchange. This was previously observed for Gd-DOTASA (H_5DOTASA = 1,4,7,10-tetraazacyclododecane-1-succinic-4,7,10-triacetic acid), where the carboxylate group is even closer to the coordination cage ($k_{ex}^{298} = (6.3 \pm 0.2) \times 10^6$ s^{-1}).[49]

Beside the effect of the negative charge of the carboxylate on the water exchange, the pending group might lead to a structural change and induce some steric crowding in the inner coordination sphere of the complex with respect to Gd-DOTA, which might also contribute to the acceleration of the water exchange. This effect is expected to increase with increasing length and rigidity of the linker. It is likely operative for **14**, where the additional negative charge is farther away from the inner sphere, and becomes even more important for Gadoxane G and B. Indeed, the Gadoxane compounds do not have an additional negative charge, and still present faster water exchange than Gd-DOTA. Another factor that might be considered when explaining the different water exchange rates is that the minor (m) and major (M) isomers of DOTA-type Ln^{3+} complexes have significantly different

(45) Powell, D. H.; Dhubhghaill, O. M. N.; Pubanz, D.; Helm, L.; Lebedev, Y. S.; Schlaepfer, W.; Merbach, A. E. *J. Am. Chem. Soc.* **1996**, *118*, 9333–9346.
(46) Rast, S.; Borel, A.; Helm, L.; Belorizky, E.; Fries, P. H.; Merbach, A. E. *J. Am. Chem. Soc.* **2001**, *123*, 2637–2644.
(47) Rast, S.; Fries, P. H.; Belorizky, E. *J. Chem. Phys.* **2000**, *113*, 8724–8735.
(48) Micskei, K.; Helm, L.; Brucher, E.; Merbach, A. E. *Inorg. Chem.* **1993**, *32*, 3844–3850.
(49) André, J. P.; Mäcke, H. R.; Tóth, É.; Merbach, A. E. *JBIC* **1999**, *4*, 341–347.

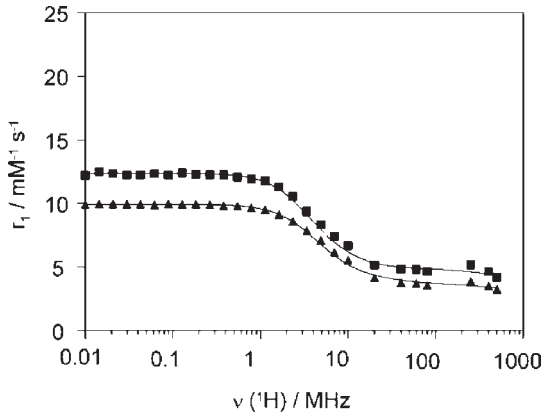

Figure 10. NMRD profile of Gd-DOTAGA (**13**) at 25 °C (■) and 37 °C (▲). The lines represent the least-squares simultaneous fit of all data points.

water exchange rate.[50] Consequently, the shift in the ratio of m/M isomers is often responsible for differences in the water exchange rate between different DOTA-type Gd^{3+} chelates.

In a second step, the NMRD profiles of all four compounds (Figures 10−13) were analyzed to yield primary information on the rotational dynamics. In these fittings, the parameters describing the water exchange (k_{ex}^{298}, $\Delta H^{\ddagger}$) were fixed to the values obtained from the fit of the ^{17}O NMR data. In addition, r_{GdH} was set to the common value of 3.10 Å based on recent electron−nuclear double resonance (ENDOR) spectroscopic results,[51,52] and the distance of closest approach of an outer-sphere water proton to Gd^{3+}, a_{GdH}, to 3.5 Å. The diffusion constant, D_{GdH}^{298}, used in the analysis of the proton NMRD data and the corresponding activation energy, E_{GdH} were adjusted to reasonable values ($D_{GdH}^{298} = 23 \times 10^{-10}$ m^2 s^{-1} and $E_{GdH} = 22$ kJ mol^{-1} for Gd-DOTAGA and Gd-DOTABA and $D_{GdH}^{298} = 26 \times 10^{-10}$ m^2 s^{-1} and $E_{GdH} = 20$ kJ mol^{-1} for Gadoxane G and Gadoxane B).

The ^1H NMRD profiles of the monomers (Figures 10 and 11) were fitted using a single rotational correlation time τ_{RH}^{298}, corresponding to the rotation of the Gd−H_{water} vector. Note that because of the internal motion of the coordinated water molecules around the Gd−O axis, τ_{RH}^{298} is usually lower than the rotational correlation time of the Gd−O_{water} vector τ_{RO}^{298} ($\tau_{RH}/\tau_{RO} = 0.65 \pm 0.2$).[53,54] The obtained values for τ_{RH}^{298} and its activation energy E_{RH}, as well as the parameters of the electron spin relaxation (τ_v^{298}, Δ^2), are depicted in Table 3.

For the two Gadoxanes, a satisfying fit of the experimental NMRD data above 10 MHz (Figures 12 and 13) could only be obtained by using the Lipari−Szabo model-free approach,[55,56] previously applied to evaluate NMR relaxation data of numerous macromolecular systems. The Lipari−Szabo approach allows the separation of two kinds of rotational motions influencing relaxation, a fast local motion being characterized by a correlation time τ_{lR}^{298} and its activation energy E_{lR}, as well as a slower global motion with a correlation time τ_{gR}^{298} (activation energy E_{gR}) (Table 3). A measure for the spatial restriction of the local motion is given by the parameter S^2. For an

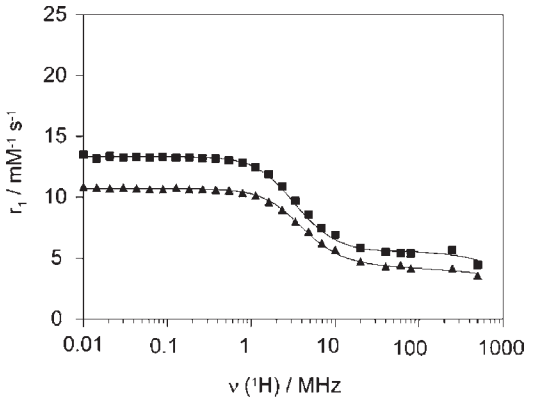

Figure 11. NMRD profile of Gd-DOTABA (**14**) at 25 °C (■) and 37 °C (▲). The lines represent the least-squares simultaneous fit of all data points.

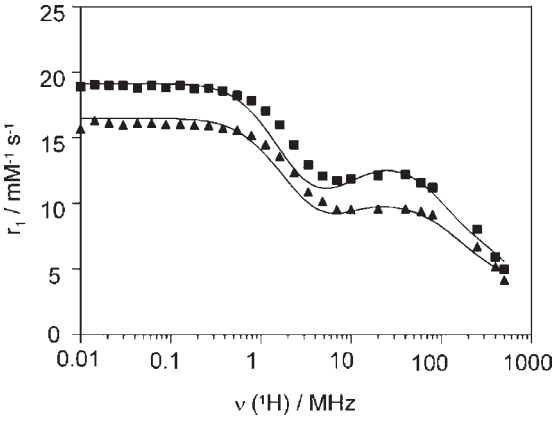

Figure 12. NMRD profiles of Gadoxane G (**GG**) at 25 °C (■) and 37 °C (▲). The lines represent the least-squares simultaneous fit of all data points.

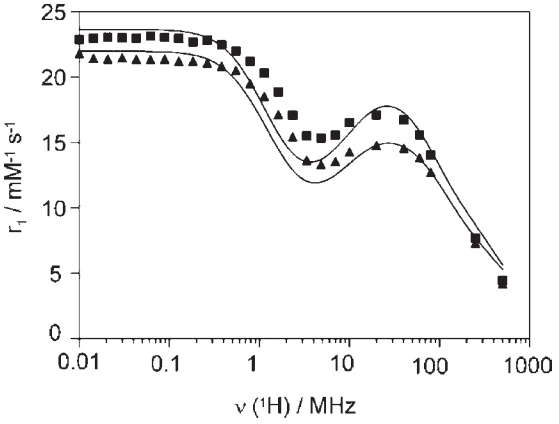

Figure 13. NMRD profiles of Gadoxane B (**GB**) at 25 °C (■) and 37 °C (▲). The lines represent the least-squares simultaneous fit of all data points.

(50) Dunand, F. A.; Aime, S.; Merbach, A. E. *J. Am. Chem. Soc.* **2000**, *122*, 1506–1512.
(51) Raitsimring, A. M.; Astashkin, A. V.; Baute, D.; Goldfarb, D.; Caravan, P. *J. Phys. Chem. A* **2004**, *108*, 7318–7323.
(52) Zech, S. G.; Sun, W.-C.; Jacques, V.; Caravan, P.; Astashkin, A. V.; Raitsimring, A. M. *ChemPhysChem* **2005**, *6*, 2570–2577.
(53) Dunand, F. A.; Borel, A.; Merbach, A. E. *J. Am. Chem. Soc.* **2002**, *124*, 710–716.
(54) Yerly, F.; Hardcastle, K. I.; Helm, L.; Aime, S.; Botta, M.; Merbach, A. E. *Chem.—Eur. J.* **2002**, *8*, 1031–1039.
(55) Lipari, G.; Szabo, A. *J. Am. Chem. Soc.* **1982**, *104*, 4559–4570.
(56) Lipari, G.; Szabo, A. *J. Am. Chem. Soc.* **1982**, *104*, 4546–4559.

Table 4. Relaxivity r_1 (at 25°C and 20 MHz) and Parameters Characterizing the Rotational Motion of Selected DOTA-Type Gadolinium Complexes

complex	τ_{lR}^{298} [ps]	τ_{gR}^{298} [ps]	S^2	τ_{RDiff}^{298} [ps]	r_1 [mM^{-1} s^{-1}]
Gd-DOTAGA (**13**)	93 ± 8[a]			139 ± 1	5.18
Gd-DOTABA (**14**)	117 ± 10[a]			183 ± 1	5.87
Gd-DOTASA[49]	125[a]				5.93
Gd-DOTA[45]	77[a]				4.74
		Dendrimers			
Gadoxane G (**GG**)	240 ± 10	1500 ± 400	0.14	3370 ± 60	12.13
Gadoxane B (**GB**)	380 ± 20	1900 ± 400	0.21	3320 ± 50	17.11
Gadomer 17[9]	760	3050	0.50		16.46
		Micelles			
Gd-DOTASA-C_{12}[13]	920[a]				18.03
Gd-DOTA-C_{12}[14]	430	1600	0.23		17.24

[a] No Lipari−Szabo treatment; a single τ_{RH}^{298} is calculated.

isotropic internal motion $S^2 = 0$, while for a fully restricted motion $S^2 = 1$ (Table 3).

Table 4 shows proton relaxivity data and rotational correlation times of our compounds presented in this work and a series of DOTA-type gadolinium complexes of various sizes, previously reported in the literature. In the case of Gd-DOTASA, the rotational correlation time τ_{RH}^{298} is about 60% larger than that of Gd-DOTA. As referred to the increased molecular weight, one would only expect an increase in τ_{RH}^{298} of about 10%, the significantly higher increase was explained by the ability of the negatively charged additional carboxylate to assemble water molecules in the second coordination sphere. They move together with the complex, thereby further increasing the rotational correlation time. The rotational correlation time τ_{RH}^{298} of Gd-DOTAGA (**13**) is also higher than that of Gd-DOTA, but with only 20% the increase is significantly smaller than for Gd-DOTASA. Because of the longer alkyl chain, the hydrophobicity of the linker is increased, thereby preventing the formation of a large second sphere hydration layer. As was already observed in the diffusion NMR study, the larger linker of Gd-DOTABA (**14**) prolongs the rotational correlation time of **14**. τ_{RH}^{298} of **14** is therefore again in the range of Gd-DOTASA. The obtained values for the rotational correlation time by the analysis of the NMRD profiles, τ_{RH}^{298}, are smaller than those obtained from the diffusion NMR studies, τ_{RDiff}^{298} (Table 1). As mentioned above, τ_{RH}^{298} corresponds to the rotation of the $Gd-H_{water}$ vector, being faster than that of the $Gd-O_{water}$ vector because of the internal rotation of the water molecule. On the contrary, τ_{RDiff}^{298} represents the global rotational motion of the whole complex. Indeed, if the τ_{RH}^{298} values determined for **13** and **14** are multiplied with the above-mentioned relation to τ_{RO}^{298}, values of 143 ± 12 ps and 180 ± 15 ps, respectively are obtained. These values are in excellent agreement with the obtained τ_{RDiff}^{298} values (139 ± 1 ps and 183 ± 1 ps for **13** and **14**, respectively). If one assumes that the τ_{RO}^{298} of these monomeric complexes match with their global rotational correlation times, these results emphasize that PGSE diffusion NMR spectroscopy is an appropriate method for determining the global rotational correlation time of such almost spherical compounds.

The effect of the longer rotational correlation times of **13** and **14** is reflected in their higher relaxivities as compared to Gd-DOTA. At 25 °C and a proton resonance frequency of 20 MHz, the relaxivity of **13** is 9% higher and the relaxivity of **14** is even 24% higher than that of Gd-DOTA. As at this field and for such small molecular weight compounds, the relaxivities are exclusively limited by the rotational correlation time, and the relaxivity of **14** is comparable to that of Gd-DOTASA despite the faster water exchange rate of the latter.

The attachment of the two monomers to the octa-(aminopropyl)silsesquoxane core results in a "high field" peak between 20 and 40 MHz in the NMRD profiles of Gadoxane G (**GG**) and Gadoxane B (**GB**) (Figures 13 and 14). This is typical of larger molecular weight MRI contrast agents, where the rotation of the gadolinium(III) chelates is substantially slowed down. As shown above, the global rotational correlation times τ_{RDiff}^{298} of **GG** and **GB** obtained by the diffusion measurements are almost the same; however, the NMRD profiles are different. For **GG**, a limited relaxivity of 12.13 mM^{-1} s^{-1} was obtained at 25 °C and a proton resonance frequency of 20 MHz. This can be related to the high flexibility of the linker and the aminopropyl group on the silsesquioxane, resulting in a short local correlation time τ_{lR}^{298} of only 240 ± 10 ps. Remarkably, the replacement of the ethyl spacer in the linking group of **GG** by a phenyl ring in **GB**, increases τ_{lR}^{298} to 380 ± 20 ps and consequently it leads to a significantly higher relaxivity (17.11 mM^{-1} s^{-1} at 25 °C and 20 MHz) for Gadoxane B. This points out that DOTABA can be in general a useful ligand for attaching stable DOTA-type complexes to (bio)macromolecules and thereby achieving high relaxivities.

The apparent global rotational correlation times of **GG** and **GB** as calculated from the NMRD profiles are 2 and 1.5 times shorter, respectively, than those obtained from the diffusion measurements. This difference can be attributed to the still relatively high flexibility of these systems. As expected, the greater rigidity of **GB** with respect to **GG** is expressed by a higher value of S^2. The relaxivity of **GB** at 20 MHz is comparable to other DOTA-type macromolecular dendrimers and micelles (Table 4). The relaxivity increase of more than 40% from **GG** to **GB** shows the potential for even higher relaxivities by further increasing the rigidity of these systems. Furthermore, both Gadoxanes show still relatively high relaxivities when going to higher magnetic fields. The relaxivity values measured at 250 MHz and 25 °C are 8.03 and 7.70 mM^{-1} s^{-1} for **GG**

and **GB**, respectively (see Supporting Information), the double of the relaxivity of Gd-DOTA (4.02 mM^{-1} s^{-1}) at the same Larmor frequency, and they are comparable to that of the much larger size dendrimer Gadomer 17 (7.88 mM^{-1} s^{-1} at 200 MHz and 25 °C).[9] This shows again, that for high field applications the development of very rigid medium-size CA is the right choice and that it is not worth further increasing the size of the CAs since it does not bring any relaxivity gain but increases the retention time of the CA in the body.

Note, that for **GG** and **GB**, the electron spin relaxation parameters obtained from ^{17}O NMR data are significantly different from those obtained by the evaluation of the ^{1}H NMRD data (Table 3). As this is related to the shortcomings of the electron spin relaxation theory used, the interpretation of these values in terms of physical meaning is not possible.

Conclusions

To obtain the novel silsesquioxane-based MRI CAs Gadoxane G (**GG**) and Gadoxane B (**GB**), we used a new route for the synthesis of DOTAGA, and developed the novel ligand DOTABA possessing a phenyl spacer. Eight lanthanide(III) complexes of DOTAGA or DOTABA could be attached to an amino-functionalized T_8-silsesquionxane to yield **GG** and **GB**, respectively, as evidenced by multinuclear NMR spectroscopy and HR-MS on the yttrium(III) and/or gadolinium(III) complexes. PGSE diffusion ^{1}H NMR measurements yielded rotational correlation times of ~3.35 ns for both **GG** and **GB**. Despite the also similar water exchange rates, the relaxivities of **GB** are significantly higher than those of **GG** over almost the whole range of magnetic fields (54% difference at 37 °C, 20 MHz). This difference arises from a higher local rotational correlation time of **GB** because of a greater rigidity, emphasizing the importance of the spacer between the core and the attached chelates.

A key issue of potential silsesquioxane-based CAs is the stability of the silsesquioxane cage toward hydrolysis in aqueous media. Frozen aqueous solutions of the Gadoxanes can be stored at −28 °C for at least 10 months without decomposition. At 25 °C and pH 7.0, a slow hydrolysis of the silsesquioxane core is observed, which is accelerated at higher temperatures. Relaxivity measurements of **GG** and **GB** were used to assess the degradation under physiological conditions (pH 7.4, 37 °C) in the presence and absence of cell culture media and fetal calf serum. The hydrolysis of the silsesquioxane core leads to smaller fragments, therefore to a reduction of r_1, while the gadolinium(III) remains safely complexed. No significant effect of the added serum on the hydrolysis rate was observed. However, the hydrolysis becomes faster with increasing pH (e.g., $t_{1/2}$ = 15 h at pH 7.4 vs for 55 min at pH 8.1 for **GG**). Intriguing is the fact that the initial breaking of Si−O−Si moieties has no effect on the relaxivity. This period of constant relaxivity (about 3 h) under physiological conditions, together with the generally accepted non-toxicity of silica monomers,[57] suggest the possibility of in vivo applications of silsesquioxane-based CAs, despite the lability of the silsesquioxane cage. Moreover, with hydrodynamic radii of ~1.44 nm, **GG** and **GB** can undergo glomerular filtration already in its intact form and should therefore be excreted relatively fast via the kidneys. However, the lability of the silsesquioxane core could even be beneficial for applications where very large dendrimeric CAs possessing numerous gadolinium centers are required to achieve high local gadolinium(III) concentrations. In these cases, the degradation of the silsesquioxane core might allow a faster clearance of the CA, or rather of its fragments, from the body.

Acknowledgment. J.H. thanks the Fonds der Chemischen Industrie for a Ph.D. scholarship. The authors thank Dr. Rolf Pohmann for providing software, sequences, and evaluation protocols for MRI measurements. This work is funded by the German Ministry for Education and Research (BMBF), FKZ 01EZ0813, and was performed in the frame of COST Action D38 "Metal-Based Systems for Molecular Imaging Applications".

Supporting Information Available: ^{1}H NMR spectra and HR mass spectra of **GG** and **GB**; longitudinal relaxivity data for **GG** and **GB** under physiological conditions; variable temperature reduced longitudinal and transverse ^{17}O relaxation rate and chemical shift data of Gd-DOTAGA, Gd-DOTABA, **GG**, and **GB** together with the least-squares fits for **GG** and **GB**; ^{1}H NMRD data of Gd-DOTAGA, Gd-DOTABA, **GG**, and **GB**; equations used in the analysis of the ^{17}O NMR and ^{1}H NMRD data. This material is available free of charge via the Internet at http://pubs.acs.org.

(57) Ilner, R. K. *The Chemistry of Silica*; Wiley: New York, 1979.